Mathematics in Applied Sciences and Engineering
Online First, pp.**1-31**

https://ojs.lib.uwo.ca/mase
https://doi.org/10.5206/mase/22708

MODELING THE IMPACT OF TREATMENT, VACCINATION AND STERILE MOSQUITO RELEASE ON MALARIA TRANSMISSION

ERIC NUMFOR

Abstract. In this study, we develop and analyze a mathematical model to investigate the effects of treatment, vaccination, and sterile male mosquito release on malaria transmission. The model incorporates different levels of immunity, distinguishing between non-immune and semi-immune populations to better capture the dynamics of malaria spread and control. Using the next-generation matrix method, we compute the control reproduction number and establish the local asymptotic stability of the disease-free equilibrium when $\mathcal{R}_C < 1$. A global sensitivity analysis with the reproduction number as the outcome variable is conducted to determine key parameters influencing malaria transmission. Additionally, we formulate and analyze an optimal control problem incorporating vaccination, treatment, and sterile male mosquito release as controls, and carry out a cost-effectiveness analysis to assess the economic feasibility of various intervention strategies. Our results suggest that a comprehensive intervention strategy that integrates treatment, vaccination, and sterile mosquito release is the most effective approach for reducing malaria transmission. However, from a cost-effectiveness perspective, prioritizing vaccination and treatment is the most feasible option in resource-limited settings.

1. Introduction

Malaria is a vector-borne disease caused by the parasite called *Plasmodium*, which is primarily transmitted to humans via bites by infected female anopheles mosquitoes. There are five species of *Plasmodium* parasites: *Plasmodium falciparum*, *Plasmodium vivax*, *Plasmodium malariae*, *Plasmodium ovale*, and *Plasmodium knowlesi* [45]. Two of the five species pose devastating threat to humans, namely, *P. falciparum* and *P. vivax*. *Plasmodium falciparum* is prevalent in sub-Saharan Africa and *P. vivax* is prevalent in Southeast Asia and South America. According to the World Health Organization (WHO), there were 263 million cases of malaria globally, resulting in an estimated 597 thousand deaths by the end of 2023 [45]. A disproportionate share of the malaria cases were observed in the African Region, with 94% of cases and 95% of deaths [45]. The symptoms of malaria can be mild or life-threatening. Mild symptoms are fever, chills, and headache, whereas severe symptoms include fatigue, confusion, seizures, difficulty breathing, jaundice, and abnormal bleeding. Pregnant women, children under five, and individuals with HIV or AIDS are at higher risk of contracting malaria. Malaria (in humans) can be controlled through treating infected individuals, vaccination of susceptible individuals and vector control. Several medications are used to treat malaria, the most common being chloroquine, primaquine, and artemisinin, with the specific medicine used depending on the individual and the species of *Plasmodium* [45]. On the other hand, vaccination is a safe and effective method of protecting individuals against harmful diseases. In 2021, WHO recommended the use of the vaccine RTS,S/AS01 among children in regions with moderate to high *P. falciparum*, and in 2023, WHO recommended a second malaria vaccine R21/Matrix-M [45]. The R21/Matrix-M vaccine represents a major milestone in the

Received by the editors 19 March 2025; accepted 31 August 2025; published online 8 September 2025.
2020 *Mathematics Subject Classification.* 92B05, 93A30, 93C15.
Key words and phrases. Malaria, wild mosquitoes, sterile mosquitoes, stability, optimal control.

global fight against malaria and has the potential to transform public health efforts in regions most affected by the disease. Finally, one of the most effective means for controlling malaria is vector control. Several methods have been used in controlling the mosquito (vector) population, some of which are the use of insecticide-treated nets (ITNs) and indoor residual spraying (IRS). However, these two methods face challenges in their implementation, such as insufficient access to and difficulty maintaining insecticide-treated nets. However, the emergence of insecticide resistance in mosquitoes and drug resistance in Plasmodium species has underscored the need for innovative control strategies.

The Sterile Insect Technique (SIT) is a biological control method that involves the release of sterile male mosquitoes into wild populations. This technique is an environmentally-friendly insect pest control method that involves sterilization, using radiation of a target pest, followed by systematic release of the sterile males, where they mate with wild females, resulting in no offspring [23]. It is assumed that when females mate with sterile males, their eggs do not hatch, leading to a reduction in the mosquito population over time. This method, when implemented effectively, offers a species-specific, environmentally friendly, and sustainable solution to malaria control. SIT has been used since the 1950s to control a variety of insecticide pests, including fruit flies, screwworm flies, and different species of mosquitoes [14]. In the United States, SIT has been used to control Aedes aegypti mosquitoes which cause dengue, Zika, and chikungunya.

In recent years, there has been a growing trend in the formulation of various models that incorporate a range of control strategies, such as the sterile insect techniques (SIT), treatment, and vaccination, to assess the effectiveness in managing the spread of malaria. These models vary in their approaches, with some focusing on individual control strategies, while others explore the outcomes of combining multiple interventions in the fight against malaria transmission. Ducrot et al. [18] developed a deterministic model that examines malaria transmission by considering two distinct human hosts (non-immune and semi-immune individuals). Their model proposed that in regions with low to moderate levels of malaria transmission, targeting control measures towards specific host types could be effective in eradicating the disease. Additionally, their results suggest that in high transmission areas where the majority of individuals originate from non-malarial regions, malaria could be eliminated by focusing on the non-immune population. In endemic areas with a low per capita birth rate or constant influx of individuals, sustained malaria control could be achieved by targeting the non-immune group. Ibrahim and Dénes [22] developed a mathematical model to study the dynamics of malaria transmission, taking into account factors such as partial immunity in humans and seasonal variations in the environment. Their model divides the human population into non-immune and semi-immune categories to account for differing levels of susceptibility. It also considers seasonal changes in mosquito birth, death, and biting rates to account for seasonal variations on transmission dynamics. On the other hand, Cai et al. [11] developed a mathematical model to assess the effectiveness of using a combination of sterile insect technique (SIT) and insecticide-treated nets (ITNs) in controlling malaria transmission. Their model comprises different sub-models for humans (SEIR) and mosquitoes (SEI), with an additional class for sterile male mosquitoes (M). Tchoumi et al.[39] formulated a two-group malaria transmission model structured by age with vaccination of individuals aged 5 and younger. Building on the work of Ibrahim and Dénes [22], Tchoumi et al. [39], and Cai et al. [11], we formulate a model for malaria in humans and mosquitoes that considers varying susceptibility levels, while incorporating vaccination against malaria, treatment and the introduction of sterile male mosquitoes into the mosquito population. This model will allow for a more comprehensive assessment of the impact of different control strategies on the dynamics of malaria transmission.

This paper is organized as follows: in Section 2, we propose a model that accounts for different levels of susceptibility, while incorporating vaccination, treatment and sterile male mosquitoes release. The

analysis of the model is presented in Section 3. The global sensitivity analysis is presented in Section 3.3, and the numerical simulations of the model are presented in Section 3.4. We formulate and analyze an optimal control problem of vaccination, treatment and sterile male mosquito release in Section 4. The numerical results of our control problem are presented in Section 4.1, and a cost-effectiveness analysis is presented in Section 5. The conclusions of our work are presented in Section 6.

2. Model Formulation

We formulate a model of malaria in humans and mosquitoes which incorporates sterile male mosquitoes, vaccination and malaria treatment. In humans, we formulate an SVEIR-type model with S, V, E, I, R representing susceptible, vaccinated, exposed, infectious and recovered humans, respectively. Based on the level of immunity, we divide the human population into two groups, namely, non-immune (i.e. those who have not developed any immunity against malaria) and semi-immune (i.e. those who have some partial immunity against malaria), denoted by the subscripts n and s, respectively. The total population of humans is

$$N_h(t) = S_n(t) + S_s(t) + E_n(t) + E_s(t) + I_n(t) + I_s(t) + V(t) + R_s(t),$$

where S_n, E_n and I_n are non-immune susceptible, exposed and infectious individuals, respectively. Similarly, S_s, E_s and I_s are semi-immune susceptible, exposed and infectious individuals, respectively, and R_s are the immune individuals. Individuals in the R_s class are partially immune to malaria, and so they harbor a small number of parasites in their bloodstream, which enables them to transmit the infection to susceptible mosquitoes [11, 16, 22, 31]. Due to vaccination of susceptible humans with malaria vaccine, we incorporate a compartment for vaccinated individuals, denoted by V. In the mosquito population, we formulate an SEIM model of malaria, where S_v, E_v and I_v represent wild (non-sterile) female mosquito populations, with S_v being those who are susceptible to malaria, E_v are individuals exposed to malaria from humans and I_v are individuals infected with malaria. We assume that M represents the sterile male mosquito population, and denote the total wild mosquito population as N_v and the total population of mosquitoes as N_{vm}, so that

$$N_v(t) = S_v(t) + E_v(t) + I_v(t) \qquad \text{and} \qquad N_{vm}(t) = N_v(t) + M(t).$$

We assume that individuals are recruited into the population through the non-immune and semi-immune susceptible classes at rate $p\Lambda_h$ and $(1-p)\Lambda_h$, respectively, where $p \in [0,1]$ is the proportion of non-immune susceptible humans recruited. When non-immune infectious humans receive malaria treatment at rate u, a fraction σ of them recovery without immunity and move to the S_n class, while the remaining individuals recover with partial immunity and move to the R_s class. Similarly, when semi-immune infectious humans receive malaria treatment at rate u, a fraction σ of them recovery with a low level of immunity and move to the S_s class, while the remaining individuals recover with partial immunity and move to the R_s. In the human population, non-immune exposed individuals progress to the infectious class at rate ψ_n, semi-immune exposed individuals progress to the infectious class at rate ψ_s, and all individuals experience a background mortality at rate μ_h. It is assumed that non-immune and semi-immune infectious humans suffer an additional disease-induced death at rates δ_n and δ_s, respectively.

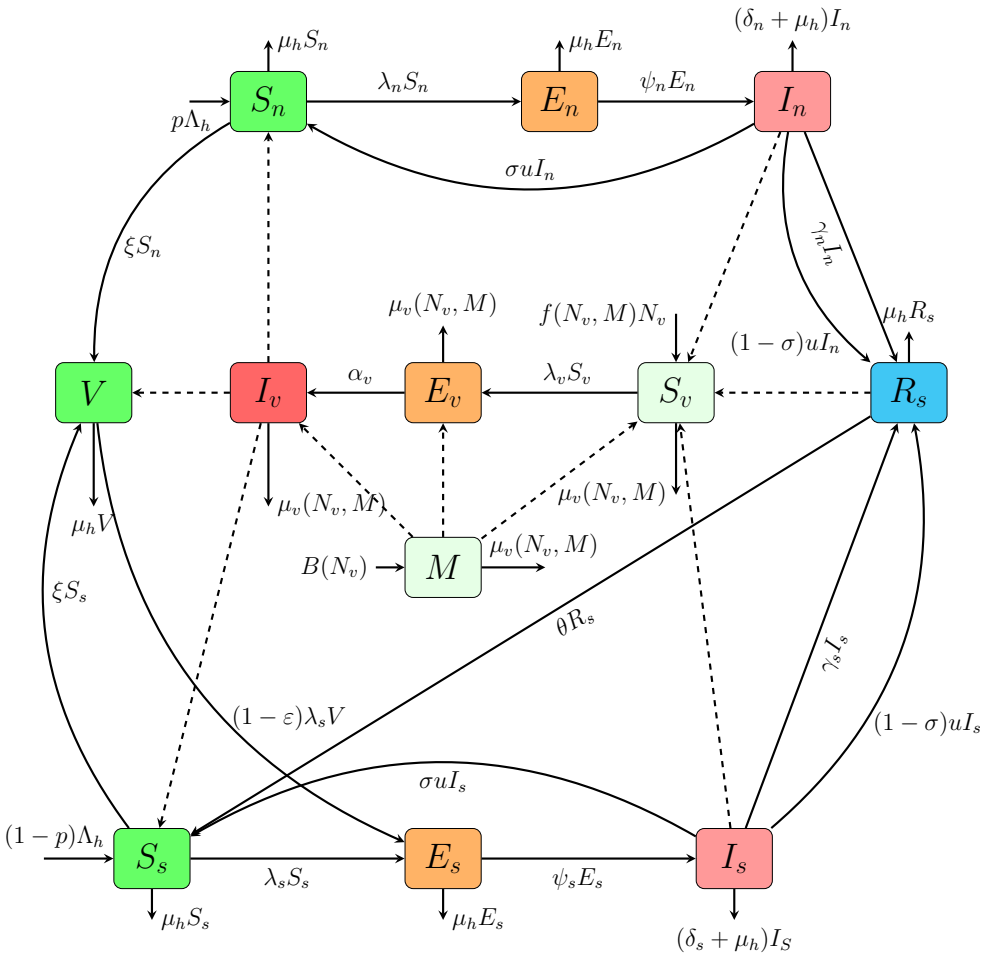

FIGURE 1. Schematic diagram of the malaria model with vaccination, treatment, and sterile male mosquito release.

When vaccinated humans come in contact with infectious mosquitoes, they become semi-immune exposed at rate $(1-\varepsilon)\lambda_s$, where λ_s is the force of infection and ε represents the efficacy of the vaccine.

In the mosquito population, we assume that all new susceptible mosquitoes are recruited at rate

$$f_v(N_v, M) \equiv f(N_v, M)N_v = \frac{aN_v}{N_v + M} N_v,$$

where a is the average number of mosquito offspring per unit time [26, 46]. In the absence of sterile mosquitoes, the birth rate f_v is proportional to N_v; the birth rate is reduced for nonzero sterile mosquito as a result of mating with wild mosquitoes. It is assumed that exposed mosquitoes become infectious at rate α_v. Furthermore, we assume that sterile mosquitoes are released at rate b proportional to the total wild population (that is, $B(N_v) = bN_V$), and that all mosquitoes (wild and sterile) suffer a background mortality at rate

$$\mu_v(N_v, M) = \mu_{1v} + \mu_{2v}(N_v + M),$$

where μ_{1v} represents density independent death, while μ_{2v} represents density-dependent death as a result of competition, overcrowding or other ecological factors. The force of infections in the non-immune population (λ_n), the semi-immune population (λ_s), and in the mosquito population (λ_v) are defined as:

$$\lambda_n = \frac{\rho_{vh} I_v}{N_h}, \qquad \lambda_s = \frac{\tilde{\rho}_{vh} I_v}{N_h}, \qquad \lambda_v = \frac{\rho_{hv} I_n}{N_h} + \frac{\tilde{\rho}_{hv} I_s}{N_h} + \frac{\hat{\rho}_{hv} R_s}{N_h}, \tag{2.1}$$

where ρ_{vh} is the transmission probability from infectious mosquitoes to non-immune susceptible humans and $\tilde{\rho}_{vh}$ is the transmission probability from infectious mosquitoes to semi-immune susceptible humans. Similarly, ρ_{hv} is the transmission probability from non-immune infectious humans to susceptible mosquitoes, $\tilde{\rho}_{hv}$ is the transmission probability from semi-immune infectious humans to susceptible mosquitoes, and $\hat{\rho}_{hv}$ is transmission probability from the immune humans (R_s) to susceptible mosquitoes. The transition rates in human and mosquito populations are represented in the schematic diagram in Figure 1. From the schematic diagram in Figure 1, we obtain the following system of nonlinear ordinary differential equations:

$$\begin{aligned}
\frac{\mathrm{d}S_n}{\mathrm{d}t} &= p\Lambda_h + \sigma u I_n - \frac{\rho_{vh} I_v S_n}{N_h} - (\mu_h + \xi) S_n, \\
\frac{dE_n}{dt} &= \frac{\rho_{vh} I_v}{N_h} S_n - (\psi_n + \mu_h) E_n, \\
\frac{dI_n}{dt} &= \psi_n E_n - (\delta_n + \gamma_n + \mu_h + u) I_n, \\
\frac{dS_s}{dt} &= (1-p)\Lambda_h + \sigma u I_s + \theta R_s - \frac{\tilde{\rho}_{vh} I_v S_s}{N_h} - (\mu_h + \xi) S_s, \\
\frac{dE_s}{dt} &= \frac{\tilde{\rho}_{vh} I_v}{N_h} S_s + (1-\varepsilon)\frac{\tilde{\rho}_{vh} I_v}{N_h} V - (\psi_s + \mu_h) E_s, \\
\frac{dI_s}{dt} &= \psi_s E_s - (\delta_s + \gamma_s + \mu_h + u) I_s, \\
\frac{dV}{dt} &= \xi(S_n + S_s) - (1-\varepsilon)\frac{\tilde{\rho}_{vh} I_v}{N_h} V - \mu_h V, \\
\frac{dR_s}{dt} &= (\gamma_n + (1-\sigma)u) I_n + (\gamma_s + (1-\sigma)u) I_s - (\theta + \mu_h) R_s, \\
\frac{dS_v}{dt} &= \frac{aN_v}{N_v + M} N_v - \left(\frac{\rho_{hv} I_n}{N_h} + \frac{\tilde{\rho}_{hv} I_s}{N_h} + \frac{\hat{\rho}_{hv} R_s}{N_h} \right) S_v - (\mu_{1v} + \mu_{2v}(N_v + M)) S_v, \\
\frac{dE_v}{dt} &= \left(\frac{\rho_{hv} I_n}{N_h} + \frac{\tilde{\rho}_{hv} I_s}{N_h} + \frac{\hat{\rho}_{hv} R_s}{N_h} \right) S_v - \alpha_v E_v - (\mu_{1v} + \mu_{2v}(N_v + M)) E_v, \\
\frac{dI_v}{dt} &= \alpha_v E_v - (\mu_{1v} + \mu_{2v}(N_v + M)) I_v, \\
\frac{dM}{dt} &= bN_v - (\mu_{1v} + \mu_{2v}(N_v + M)) M,
\end{aligned} \tag{2.2}$$

with initial population

$$\begin{aligned}
&S_n(0) = S_n^0, \quad E_n(0) = E_n^0, \quad I_n(0) = I_n^0, \\
&S_s(0) = S_s^0, \quad E_s(0) = E_s^0, \quad I_s(0) = I_s^0, \\
&R_s(0) = R_s^0, \quad V(0) = V^0, \quad M(0) = M^0, \\
&S_v(0) = S_v^0, \quad E_v(0) = E_v^0, \quad I_v(0) = I_v^0.
\end{aligned} \tag{2.3}$$

A summary of the description of the parameters of model (2.2) and their values is given in Table 1.

Table 1: Description of parameters of model (2.2). The sterile mosquito release rate satisfies $a > b + \mu_{1v}$, based on biological feasibility of the disease-free equilibrium in equation (3.2).

Para	Description	Value(s)	Source(s)
Λ_h	Recruitment rate of humans	$10^4/(55 \times 365)$	[30, 34]
μ_h	Background mortality of humans	$1/(55 * 365)$	[30, 34]
δ_n	Malaria-induced death rate of non-immune humans	0.00009	[11]
δ_s	Malaria-induced death rate of semi-immune humans	0.00009	[11]
γ_n, γ_s	Recovery rate of non-immune and semi-immune humans from malaria	0.0035 - 0.005	[11]
ψ_n	Progression rate of non-immune humans from exposed to infectious	0.1033	[39]
ψ_s	Progression rate of semi-immune humans from exposed to infectious	0.0833	[5]
μ_{1v}	Density-independent death rate of mosquitoes	0.033	[11]
μ_{2v}	Density-dependent death rate of mosquitoes	0.00002	[11]
a	Birth rate of wild mosquitoes	0.13	[11]
b	Release rate of sterile male mosquitoes	$[0, 0.097)$	Calculation
σ	Proportion of treated infectious humans who recover without immunity	0.4	[30, 34]
u	Rate of treatment of malaria in humans	[0,1)	Vary
ξ	Rate of vaccination against malaria	[0,1)	Vary
θ	Rate of loss of immunity	0.00055	[11, 18]
ε	Vaccine efficacy	$[0, 1]$	Vary
p	Proportion of non-immune susceptible humans recruited	0.5	[18]
ρ_{vh}	Transmission probability from infectious mosquitoes to non-immune susceptible humans	0.022	[11, 30, 34]
$\tilde{\rho}_{vh}$	Transmission probability from infectious mosquitoes to semi-immune susceptible humans	0.011	Estimation
ρ_{hv}	Transmission probability from non-immune infectious humans to susceptible mosquitoes	0.48	[11, 30, 34]
$\tilde{\rho}_{hv}$	Transmission probability from semi-immune infectious humans to susceptible mosquitoes	0.048	Estimation
$\hat{\rho}_{hv}$	Transmission probability from immune (R_s) humans to susceptible mosquitoes	0.048	[11]
α_v	Progression rate from exposed to infectious mosquitoes	0.091	[5, 39]

3. Mathematical Analysis

In this section, we establish the positivity and boundedness of solutions of system (2.2), compute the control reproduction number, and establish the existence and local stability of the disease-free equilibrium.

3.1. **Positivity and Boundedness.**

It is important to establish the positivity and boundedness of solutions of system (2.2), since the state variables in our model represent populations.

Theorem 3.1. *Given the positive initial conditions in equation (2.3), the solutions* $(S_n, E_n, I_n, S_s, E_s, I_s, V, R_s) \in \mathbb{R}^8_+$ *and* $(S_v, E_v, I_v, M) \in \mathbb{R}^4_+$ *of model (2.2) remain positive for all* $t \geq 0$.

Proof. Considering our state equations in (2.2), we have:

$$\begin{aligned}
\left.\frac{dS_n}{dt}\right|_{S_n=0} &= \Lambda_h + \sigma u I_n > 0, & \left.\frac{dV}{dt}\right|_{V=0} &= \xi(S_n + S_s) > 0,\\
\left.\frac{dE_n}{dt}\right|_{E_n=0} &= \lambda_n S_n > 0, & \left.\frac{dR_s}{dt}\right|_{R_s=0} &= (\gamma_n + (1-\sigma)u)I_n + (\gamma_s + (1-\sigma)u)I_s > 0,\\
\left.\frac{dI_n}{dt}\right|_{I_n=0} &= \psi_n E_n > 0, & \left.\frac{dS_v}{dt}\right|_{S_v=0} &= \frac{a(E_v+I_v)^2}{E_v+I_v+M} > 0,\\
\left.\frac{dS_s}{dt}\right|_{S_s=0} &= (1-p)\Lambda_h + \sigma u I_s + \theta R_s > 0, & \left.\frac{dE_v}{dt}\right|_{E_v=0} &= \lambda_v S_v > 0,\\
\left.\frac{dE_s}{dt}\right|_{E_s=0} &= \lambda_s S_s + (1-\varepsilon)\lambda_s V > 0, & \left.\frac{dI_v}{dt}\right|_{I_v=0} &= \alpha_v E_v > 0,\\
\left.\frac{dI_s}{dt}\right|_{I_s=0} &= \psi_s E_s > 0, & \left.\frac{dM}{dt}\right|_{M=0} &= bN_v > 0.
\end{aligned}$$

It follows from Manisha and Anuj [32], and Smith [37] that the state solutions are non-negative for all $t \geq 0$. □

Theorem 3.2. *The set*

$$\Omega = \left\{ (S_n, E_n, I_n, S_s, E_s, I_s, V, R_s, S_v, E_v, I_v, M) \in \mathbb{R}^{12}_+ \middle| 0 \leq N_h(t) \leq \mathcal{D}_1, 0 \leq N_v(t) + M(t) \leq \mathcal{D}_2 \right\}$$

is positively invariant for system (2.2), where $\mathcal{D}_1 = \max\left\{N_h(0), \frac{\Lambda_v}{\mu_h}\right\}$ *and* $\mathcal{D}_2 = \frac{a+b}{\mu_{2v}}$.

Proof. Since the total human population at time t is $N_h(t) = S_n(t) + S_s(t) + E_n(t) + E_s(t) + I_n(t) + I_s(t) + V(t) + R_s(t)$, it follows that the dynamics of the total human population satisfies

$$\frac{dN_h}{dt} = \Lambda_h - \mu_h N_h - \delta_n I_n - \delta_s I_s \leq \Lambda_h - \mu_h N_h, \tag{3.1}$$

by Theorem 3.1. Since the total population is endowed with the initial condition $N_h(0) = N_h^0$ from equation (2.3), it follows that the differential inequality (3.1) satisfies

$$0 \leq N_h(t) \leq N_h^0 e^{-\mu_h t} + \frac{\Lambda_h}{\mu_h}\left(1 - e^{-\mu_h t}\right) \leq \max\left\{N_h^0, \frac{\Lambda_h}{\mu_h}\right\} := \mathcal{D}_1,$$

by convexity. Taking into account the total population of wild mosquitoes, $N_v = S_v + E_v + I_v$, and the total population of wild and sterile mosquitoes, $N_{vm} = N_v + M$, we have $0 < N_v \leq N_{vm}$. It follows that

$$\begin{aligned}\frac{dN_{vm}}{dt} &= bN_v + \frac{aN_v^2}{N_{vm}} - (\mu_{1v} + \mu_{2v}N_{vm})N_{vm} \\ &\leq (a+b)N_{vm}\left(1 - \frac{N_{vm}}{\mathcal{D}_2}\right),\end{aligned}$$

where $\mathcal{D}_2 = \frac{a+b}{\mu_{2v}}$. Given that $N_{vm}(0) = N_{vm}^0$, it follows from the differential inequality that

$$N_{vm}(t) \leq \frac{\mathcal{D}_2 N_{vm}^0}{N_{vm}^0 + (\mathcal{D}_2 - N_{vm}^0)e^{-(a+b)t}} \to \mathcal{D}_2,$$

as $t \to \infty$. Thus, $\limsup_{t\to\infty} N_{vm}(t) \leq \mathcal{D}_2$, and hence, the set Ω is positively invariant for system (2.2). □

3.2. **Equilibria and Reproduction Number.** We determine the disease-free equilibrium (DFE) for our malaria model, which will be used in computing the reproduction number. In the absence of malaria in the population, $E_n = E_s = E_v = I_n = I_s = I_v = 0$. Thus, the disease-free equilibrium is $\mathcal{E}_0 = (S_n^*, E_n^*, I_n^*, S_s^*, E_s^*, I_s^*, V^*, R_s^*, S_v^*, E_v^*, I_v^*, M^*)$, where

$$\mathcal{E}_0 = \left(\frac{p\Lambda_h}{\mu_h+\xi}, 0, 0, \frac{(1-p)\Lambda_h}{\mu_h+\xi}, 0, 0, \frac{\xi\Lambda_h}{\mu_h(\mu_h+\xi)}, 0, \frac{(a-b)(a-b-\mu_{1v})}{a\mu_{2v}}, 0, 0, \frac{b(a-b-\mu_{1v})}{a\mu_{2v}}\right), \quad (3.2)$$

with $a > b + \mu_{1v}$. In the absence of sterile mosquitoes in the population, the disease-free equilibrium is $\tilde{\mathcal{E}}_0 = \mathcal{E}_0|_{b=0}$. In the computation of the reproduction number, we determine the vector of appearance of new infections ($\mathcal{F}$), and the vector of other transitions ($\mathcal{V}$) in the population, where we have ordered the "disease compartments" as $(E_n, I_n, E_s, I_s, R_s, E_v, I_v)$. Thus,

$$\mathcal{F} = \begin{pmatrix} \lambda_n S_n \\ 0 \\ \lambda_s S_s + (1-\varepsilon)\lambda_s V \\ 0 \\ 0 \\ \lambda_v S_v \\ 0 \end{pmatrix}, \quad \mathcal{V} = \begin{pmatrix} (\psi_n + \mu_h)E_n \\ (\delta_n + \gamma_n + \mu_h + u)I_n - \psi_n E_n \\ (\psi_s + \mu_h)E_s \\ (\delta_s + \gamma_s + \mu_h + u)I_s - \psi_s E_s \\ (\theta + \mu_h)R_s - (\gamma_n + (1-\sigma)u)I_n - (\gamma_s + (1-\sigma)u)I_s \\ \alpha_v E_v + (\mu_{1v} + \mu_{2v}(N_v + M))E_v \\ (\mu_{1v} + \mu_{2v}(N_v + M))I_v - \alpha_v E_v \end{pmatrix}.$$

For the sake of simplicity, we introduce the notation $K_1 = \delta_n + \gamma_n + \mu_h + u$, $K_2 = \delta_s + \gamma_s + \mu_h + u$, $K_3 = \gamma_n + (1-\sigma)u$, $K_4 = \gamma_s + (1-\sigma)u$ and $\mu_v(N_v^*, M^*) = \mu_{1v} + \mu_{2v}(N_v^* + M^*)$. The matrices $\mathbb{F}$ and $\mathbb{V}$ are obtained from the vectors $\mathcal{F}$ and $\mathcal{V}$ by taking the partial derivatives of $\mathcal{F}$ and $\mathcal{V}$ with respect to each "disease compartment" and evaluating at the disease-free equilibrium $\mathcal{E}_0$. Thus, the next-generation matrix is

$$\mathbb{F}\mathbb{V}^{-1} = \begin{pmatrix} 0 & 0 & 0 & 0 & 0 & \frac{\alpha_v \rho_{vh} S_n^*}{\mu_v(N_v^*,M^*)(\alpha_v + \mu_v(N_v^*,M^*))N_h^*} & \frac{\rho_{vh} S_n^*}{\mu_v(N_v^*,M^*)N_h^*} \\ 0 & 0 & 0 & 0 & 0 & 0 & 0 \\ 0 & 0 & 0 & 0 & 0 & \frac{\alpha_v \tilde{\rho}_{vh}(S_s^* + (1-\varepsilon)V^*)}{\mu_v(N_v^*,M^*)(\alpha_v + \mu_v(N_v^*,M^*))N_h^*} & \frac{\tilde{\rho}_{vh}(S_s^* + (1-\varepsilon)V^*)}{\mu_v(N_v^*,M^*)N_h^*} \\ 0 & 0 & 0 & 0 & 0 & 0 & 0 \\ 0 & 0 & 0 & 0 & 0 & 0 & 0 \\ A_1 & A_2 & A_3 & A_4 & A_5 & 0 & 0 \\ 0 & 0 & 0 & 0 & 0 & 0 & 0 \end{pmatrix},$$

where

$$\begin{aligned} A_1 &= \frac{S_v^*}{N_h^*}\left[\frac{\rho_{hv}\psi_n}{K_1(\psi_n+\mu_h)}+\frac{\hat{\rho}_{hv}K_3\psi_n}{K_1(\psi_n+\mu_h)(\theta+\mu_h)}\right], \qquad A_2=\frac{S_v^*}{N_h^*}\left[\frac{\rho_{hv}}{K_1}+\frac{\hat{\rho}_{hv}K_3}{K_1(\theta+\mu_h)}\right], \\ A_3 &= \frac{S_v^*}{N_h^*}\left[\frac{\tilde{\rho}_{hv}\psi_s}{K_2(\psi_s+\mu_h)}+\frac{\hat{\rho}_{hv}K_4\psi_s}{K_2(\psi_s+\mu_h)(\theta+\mu_h)}\right], \qquad A_4=\frac{S_v^*}{N_h^*}\left[\frac{\tilde{\rho}_{hv}}{K_2}+\frac{\hat{\rho}_{hv}K_4}{K_2(\theta+\mu_h)}\right], \\ A_5 &= \frac{\hat{\rho}_{hv}S_v^*}{(\theta+\mu_h)N_h^*}. \end{aligned}$$

The control reproduction number is

$$\mathcal{R}_C=\rho(\mathbb{F}\mathbb{V}^{-1})=\sqrt{\tilde{\mathcal{R}}_{0n}+\hat{\mathcal{R}}_{0s}}, \tag{3.3}$$

where $\tilde{\mathcal{R}}_{0n}$ and $\hat{\mathcal{R}}_{0s}$ are

$$\begin{aligned} \tilde{\mathcal{R}}_{0n} &= \frac{\alpha_v\rho_{vh}p\mu_h^2\psi_n(a-b-\mu_{1v})}{a\Lambda_h\mu_{2v}(\mu_h+\xi)(\psi_n+\mu_h)(\alpha_v+a-b)(\delta_n+\gamma_n+\mu_h+u)}\left[\rho_{hv}+\frac{\hat{\rho}_{hv}K_3}{\theta+\mu_h}\right], \\ \hat{\mathcal{R}}_{0s} &= \frac{\alpha_v\tilde{\rho}_{vh}\mu_h\psi_s(a-b-\mu_{1v})[(1-p)\mu_h+(1-\varepsilon)\xi]}{a\Lambda_h\mu_{2v}(\mu_h+\xi)(\psi_s+\mu_h)(\alpha_v+a-b)(\delta_s+\gamma_s+\mu_h+u)}\left[\tilde{\rho}_{hv}+\frac{\hat{\rho}_{hv}K_4}{\theta+\mu_h}\right]. \end{aligned}$$

The term, $\tilde{\mathcal{R}}_{0n}$, in the control reproduction number represents the number of secondary infections obtained when one infected non-immune human is introduced in a completely susceptible population during individual's entire period of infectiousness. Similarly, $\tilde{\mathcal{R}}_{0s}$ represents the number of secondary infections obtained when one infected semi-immune human is introduced in a completely susceptible population during the individual's entire period of infectiousness.

Theorem 3.3. *The disease-free equilibrium $\mathcal{E}_0$ is locally asymptotically stable if $\mathcal{R}_C<1$ and unstable if $\mathcal{R}_C>1$.*

Proof. The Jacobian matrix $J=J(\mathcal{E}_0)$ of system (2.2) at the disease-free equilibrium, $\mathcal{E}_0$ given by

$$\begin{pmatrix} -B_0 & 0 & \sigma u & 0 & 0 & 0 & 0 & 0 & 0 & 0 & \frac{-\mu_h p\rho_{vh}}{\mu_h+\xi} & 0 \\ 0 & -B_2 & 0 & 0 & 0 & 0 & 0 & 0 & 0 & 0 & \frac{\mu_h p\rho_{vh}}{\mu_h+\xi} & 0 \\ 0 & \psi_n & -K_1 & 0 & 0 & 0 & 0 & 0 & 0 & 0 & 0 & 0 \\ 0 & 0 & 0 & -B_0 & 0 & \sigma u & 0 & \theta & 0 & 0 & -B_6 & 0 \\ 0 & 0 & 0 & 0 & -B_3 & 0 & 0 & 0 & 0 & 0 & B_1 & 0 \\ 0 & 0 & 0 & 0 & \psi_s & -K_2 & 0 & 0 & 0 & 0 & 0 & 0 \\ \xi & 0 & 0 & \xi & 0 & 0 & -\mu_h & 0 & 0 & 0 & -B_7 & 0 \\ 0 & 0 & K_3 & 0 & 0 & K_4 & 0 & -B_4 & 0 & 0 & 0 & 0 \\ 0 & 0 & -\rho_{hv}B_8 & 0 & 0 & -\tilde{\rho}_{hv}B_8 & 0 & -\hat{\rho}_{hv}B_8 & -B_9 & B_{10} & B_{10} & -B_{11} \\ 0 & 0 & \rho_{hv}B_8 & 0 & 0 & \tilde{\rho}_{hv}B_8 & 0 & \hat{\rho}_{hv}B_8 & 0 & -B_{12} & 0 & 0 \\ 0 & 0 & 0 & 0 & 0 & 0 & 0 & 0 & 0 & \alpha_v & b-a & 0 \\ 0 & 0 & 0 & 0 & 0 & 0 & 0 & 0 & B_5 & B_5 & B_5 & B_5-a \end{pmatrix},$$

with

$$B_0=\mu_h+\xi, \qquad B_1=\frac{\tilde{\rho}_{vh}[(1-p)\mu_h+(1-\varepsilon)\xi]}{\mu_h+\xi}, \qquad B_2=\psi_n+\mu_h, \qquad B_3=\psi_s+\mu_h,$$
$$B_4=\theta+\mu_h, \qquad B_5=\frac{b(b+\mu_{1v})}{a}, \qquad B_6=\frac{(1-p)\mu_h\tilde{\rho}_{vh}}{\mu_h+\xi},$$
$$B_7=\frac{\tilde{\rho}_{vh}(1-\varepsilon)\xi}{\mu_h+\xi}, \qquad B_8=\frac{\mu_h}{\Lambda_h}S_V^*, \qquad B_9=\frac{(a-b)(a-2b-\mu_{1v})}{a},$$
$$B_{10}=\frac{(a-b)(2b+\mu_{1v})}{a}, \qquad B_{11}=\frac{(a-b)(2a-2b-\mu_{1v})}{a}, \qquad B_{12}=a-b+\alpha_v.$$

It follows from $a>b+\mu_{1v}$ that $B_i>0$, for $i=1,2,\cdots,12$, except for B_9. Now, we determine the eigenvalues of the Jacobian matrix, $J(\mathcal{E}_0)$. Clearly, $\lambda_1=-\mu_h<0$ and $\lambda_{2,3}=-B_0<0$ (of multiplicity 2) are eigenvalues of J. The remaining eigenvalues are obtained from the 2×2 block matrix

$$H=\left[\begin{array}{c:c} D & E \\ \hdashline F & G \end{array}\right],$$

where

$$D = \begin{pmatrix} -B_2 & 0 & 0 & 0 & 0 \\ \psi_n & -K_1 & 0 & 0 & 0 \\ 0 & 0 & -B_3 & 0 & 0 \\ 0 & 0 & \psi_s & -K_2 & 0 \\ 0 & K_3 & 0 & K_4 & -B_4 \end{pmatrix}, \qquad E=\begin{pmatrix} 0 & 0 & \frac{\mu_h p\rho_{vh}}{\mu_h+\xi} & 0 \\ 0 & 0 & 0 & 0 \\ 0 & 0 & B_1 & 0 \\ 0 & 0 & 0 & 0 \\ 0 & 0 & 0 & 0 \end{pmatrix},$$

$$F = \begin{pmatrix} 0 & -\rho_{hv}B_8 & 0 & -\tilde{\rho}_{hv}B_8 & -\hat{\rho}_{hv}B_8 \\ 0 & \rho_{hv}B_8 & 0 & \tilde{\rho}_{hv}B_8 & \hat{\rho}_{hv}B_8 \\ 0 & 0 & 0 & 0 & 0 \\ 0 & 0 & 0 & 0 & 0 \end{pmatrix}, \quad G=\begin{pmatrix} -B_9 & B_{10} & B_{10} & -B_{11} \\ 0 & -B_{12} & 0 & 0 \\ 0 & \alpha_v & b-a & 0 \\ B_5 & B_5 & B_5 & B_5-a \end{pmatrix}.$$

The eigenvalues of D are $\lambda_4=-B_2<0$, $\lambda_5=-K_1<0$, $\lambda_6=-B_3<0$, $\lambda_7=-K_2<0$, and $\lambda_8=-B_4<0$, since B_2, B_3, B_4, K_1 and K_2 are positive. Due to the invertibility of D (as $\det(D)=-B_2B_3B_4K_1K_2\neq 0$), the local stability of $\mathcal{E}_0$ is determined by the eigenvalues of the Schur complement of D, denoted by S_D and defined as $S_D=G-FD^{-1}E$ [3, 33, 38], where

$$S_D=\begin{pmatrix} -B_9 & B_{10} & B_{10}-\frac{B_8\mu_h p\psi_n\rho_{vh}}{B_2K_1(\mu_h+\xi)}\left[\frac{K_3\hat{\rho}_{hv}}{B_4}+\rho_{hv}\right]-\frac{B_1B_8\psi_s}{B_3K_2}\left[\tilde{\rho}_{hv}+\frac{\hat{\rho}_{hv}K_4}{B_4}\right] & -B_{11} \\ 0 & -B_{12} & \frac{B_8\mu_h p\psi_n\rho_{vh}}{B_2K_1(\mu_h+\xi)}\left[\frac{K_3\hat{\rho}_{hv}}{B_4}+\rho_{hv}\right]+\frac{B_1B_8\psi_s}{B_3K_2}\left[\tilde{\rho}_{hv}+\frac{\hat{\rho}_{hv}K_4}{B_4}\right] & 0 \\ 0 & \alpha_v & b-a & 0 \\ B_5 & B_5 & B_5 & B_5-a \end{pmatrix}.$$

Thus, we study the characteristic polynomial $q(\lambda)=\det(\lambda I_4-S_D)$. To do this, we introduce the notation

$$X = \frac{B_8\mu_h p\psi_n\rho_{vh}}{B_2K_1(\mu_h+\xi)}\left[\frac{K_3\hat{\rho}_{hv}}{B_4}+\rho_{hv}\right], \qquad W=(a-B_5)B_9+B_5B_{11},$$
$$Y = \frac{B_1B_8\psi_s}{B_3K_2}\left[\tilde{\rho}_{hv}+\frac{\hat{\rho}_{hv}K_4}{B_4}\right], \qquad Z=(a-b)B_{12}-\alpha_v(X+Y),$$

where by direct substitution, $W:=(a-B_5)B_9+B_5B_{11}=\frac{(a-b)^2}{a}\left[a-b-\mu_{1v}\right]>0$ and $Z=(a-b)(\alpha_v+a-b)(1-\mathcal{R}_C^2)$. Thus, the characteristic polynomial of S_D is

$$q(\lambda)=\det(\lambda I_4-S_D)\equiv\lambda^4+a_1\lambda^3+a_2\lambda^2+a_3\lambda+a_4,$$

where

$$\begin{aligned} a_1 &= -tr(S_D) = a - b + B_{12} + a - B_5 + B_9, \\ a_2 &= (a - b + B_{12})(a - B_5 + B_9) + W + Z, \\ a_3 &= (a - b + B_{12})W + (a - B_5 + B_9)Z, \\ a_4 &= \det(S_D) = WZ. \end{aligned}$$

The coefficient $a_4 := WZ = (a-b)(\alpha_v + a - b)W(1 - \mathcal{R}_C^2)$ and the term

$$a - B_5 + B_9 = \frac{a^2 - b(b + \mu_{1v}) + (a-b)(a - b - \mu_{1v}) - b(a-b)}{a} > \frac{b(a - b - \mu_{1v})}{a} > 0,$$

since $a > b > 0$. Thus, the coefficients a_1, a_2, a_3 and a_4 are positive whenever $\mathcal{R}_C < 1$. Now, $D_1 = a_1 > 0$,

$$\begin{aligned} D_2 &= a_1 a_2 - a_3 \\ &= [(a - b + B_{12}) + (a - B_5 + B_9)][(a - b + B_{12})(a - B_5 + B_9) + W + Z] \\ &\quad -[(a - b + B_{12})W + (a - B_5 + B_9)Z] \\ &= (a - b + B_{12})[Z + (a - B_5 + B_9)^2] + (a - B_5 + B_9)[W + (a - b + B_{12})^2] > 0, \end{aligned}$$

whenever $\mathcal{R}_C < 1$. Finally, if $\mathcal{R}_C < 1$,

$$\begin{aligned} D_3 &= a_1 a_2 a_3 - a_1^2 a_4 - a_3^2 \\ &= [(a - b + B_{12}) + (a - B_5 + B_9)] \cdot [(a - b + B_{12})(a - B_5 + B_9) + W + Z] \cdot \\ &\quad \cdot [(a - b + B_{12})W + (a - B_5 + B_9)Z] \\ &\quad -[(a - b + B_{12}) + (a - B_5 + B_9)]^2 WZ - [(a - b + B_{12})W + (a - B_5 + B_9)Z]^2 \\ &= (a - b + B_{12})^3 (a - B_5 + B_9)W \\ &\quad +(a - b + B_{12})^2 (a - B_5 + B_9)^2 (W + Z) + (a - b + B_{12})(a - B_5 + B_9)^3 Z \\ &\quad +(a - b + B_{12})(a - B_5 + B_9)^3 (Z - W)^2 > 0. \end{aligned}$$

Thus, the Routh-Hurwitz conditions hold and hence the disease-free equilibrium is locally asymptotically stable when $\mathcal{R}_C < 1$ [28, 29]. When $\mathcal{R}_C > 1$, the coefficient $a_4 < 0$, resulting in a change of sign in the coefficients of the polynomial q. This depicts the existence of a positive root, by Descartes Rule of Signs [2, 35]. Thus, $\mathcal{E}_0$ is unstable when $\mathcal{R}_C > 1$. □

3.3. **Sensitivity Analysis.** Partial Rank Correlation Coefficients (PRCCs) are widely used in sensitivity analysis, especially within the realm of mathematical and computational modeling. These coefficients quantify the magnitude and direction of the relationship between model inputs (parameters) and outputs (variables), while accounting for the effects of other variables. PRCCs are especially useful in models with nonlinear and monotonic relationships, making them a preferred technique in biological, epidemiological, and engineering studies. Thus, we carry out sensitivity analysis of our parameters using the latin hypercube sampling (LHS) technique. Uncertainty in model parameters can be identified through the latin hypercube sampling technique, coupled with Partial Rank Correlation Coefficients (PRCCs). Latin hypercube sampling is a scheme for simulating random parameter sets that adequately cover the parameter space [4, 10, 27, 34, 44].

In order to assess the relationship between our model parameters and the number of secondary cases ($\mathcal{R}_C$), we assume that each uncertain parameter is uniformly distributed within 25% of the respective baseline parameter values, and perform a latin hypercube sampling analysis by generating 5000 random samples from the chosen parameter distributions. Scatter plots of each parameter against the output

variable above were generated to ascertain the assumption of monotonicity, which is necessary when using PRCCs. PRCCs were then calculated between each of the following parameters: a, b, α_v, ξ, p, θ, σ, γ_n, γ_s, u, ε, Λ_h, μ_h, δ_n, δ_s, ψ_n, ψ_s, μ_{1v}, μ_{2v}, ρ_{vh}, ρ_{hv}, $\tilde{\rho}_{vh}$, $\tilde{\rho}_{hv}$ and $\hat{\rho}_{hv}$. The sign of the PRCCs indicates whether or not variations in the input parameter has a positive or negative effect on the corresponding output variable [42, 43]. The most influential parameters of the model are those that have PRCC values that satisfy $|PRCC| > 0.4$, where a negative sign indicates an inverse relationship. The correlation between the output variable and the input parameters is moderate if $0.2 < |PRCC| < 0.4$, and is weak otherwise [4, 13].

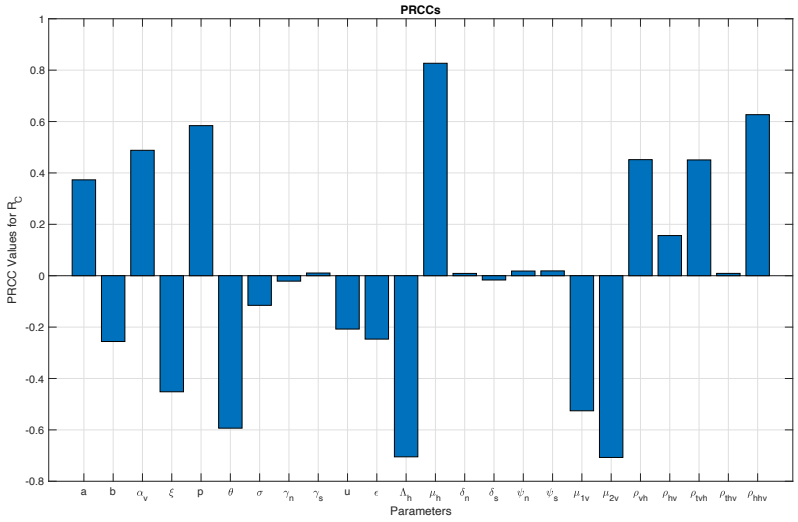

FIGURE 2. Sensitivity analysis depicting the PRCC values of the control reproduction number $\mathcal{R}_C$. In this figure, we used the following notation: $\rho_{tvh} = \tilde{\rho}_{vh}$, $\rho_{thv} = \tilde{\rho}_{hv}$ and $\rho_{hhv} = \hat{\rho}_{hv}$.

In Figure 2, besides the natural death rate μ_h, the parameters α_v, p, μ_h, ρ_{vh}, $\tilde{\rho}_{vh}$ and $\hat{\rho}_{vh}$ have the greatest impact on increasing the control reproduction number, whereas a is moderately impactful. On the other hand, besides Λ, the parameters ξ, θ, σ, ε, μ_{1v}, and μ_{2v} have the greatest impact on reducing the reproduction number, and the sterile release rate (b), treatment rate (u) and efficacy of the vaccine (ε) are moderately impactful.

3.4. **Numerical Simulations.** In this section, we explore the effects of sterile male mosquitoes release, vaccination and treatment on the spread of malaria in humans and mosquitoes. For the baseline parameter values in Table 1, and in the absence of treatment, vaccination and sterile male mosquito release, the reproduction number is $\mathcal{R}_C = 2.2$.

3.4.1. *Effect of Sterile Male Mosquito Release.* We investigate the effect of sterile male mosquitoes release under different scenarios, namely, the absence of both treatment and vaccination, presence of treatment but the absence of vaccination, presence of vaccination but the absence of treatment, and in the presence of both treatment and vaccination.

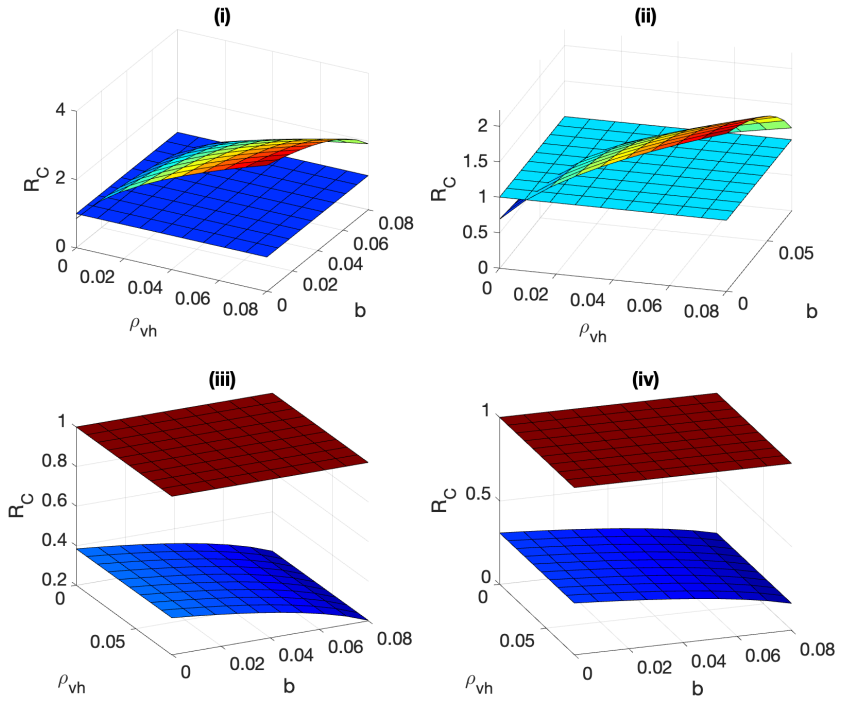

FIGURE 3. Surface plots of the control reproduction number as a function of the transmission probability from infectious mosquitoes to susceptible humans and the sterile male mosquito release rate, when (i) $u = 0$ and $\xi = 0$, (ii) $u > 0$ and $\xi = 0$, (iii) $\xi > 0$ and $u = 0$, (iv) $u > 0$ and $\xi > 0$.

Figure 3 is a surface plot for the control reproduction number as a function of the sterile male mosquito release rate (b) and the transmission probability (ρ_{vh}) from infectious mosquitoes to susceptible humans. Simulations in the absence of both treatment and vaccination are depicted in Figure 3 (i), and they suggest that the control reproduction number is below one for a very small transmission probability from infectious mosquitoes to susceptible humans, irrespective of the release rate $b \in [0, 0.08]$. When individuals receive malaria treatment, but in the absence of vaccination against malaria, the surface plot indicates that the reproduction number is above one when $\rho_{vh} > 0.02$ and $b < 0.04$, and when $b > 0.05$, $\mathcal{R}_C > 1$ whenever $\rho_{vh} > 0.04$ as in Figure 3 (ii). In the presence of vaccination, but with no treatment of malaria in humans, the surface plot of the reproduction number suggests that the control reproduction number is between 0.2 and 0.4, irrespective of the release rate $b \in [0, 0.08]$ and transmission probability ρ_{vh}, as shown in Figure 3 (iii). Finally, when humans receive malaria treatment and are vaccinated, the reproduction number is below 0.3 as shown in Figure 3 (iv). Thus, a combination of vaccination and treatment in the presence of sterile male mosquito release is more impactful at reducing malaria prevalence than vaccination-only in the presence of sterile male mosquito release as depicted in Figure 3 (iii) & (iv).

Figure 4 delineates the control reproduction number for different values of the sterile release rate. When $b = 0$ and for significantly small transmission probability from infectious mosquitoes to susceptible humans (ρ_{vh}), the control reproduction is below one and immediately exceeds one with an increase in the transmission probabilities ($\rho_{vh} > 0.0015$) as shown in Figure 4. As the sterile release rate increases,

the control reproduction number decreases, and it requires a higher transmission rate for malaria to persist in the population. This highlights the importance of sterile male mosquitoes in curbing the spread of malaria in the population.

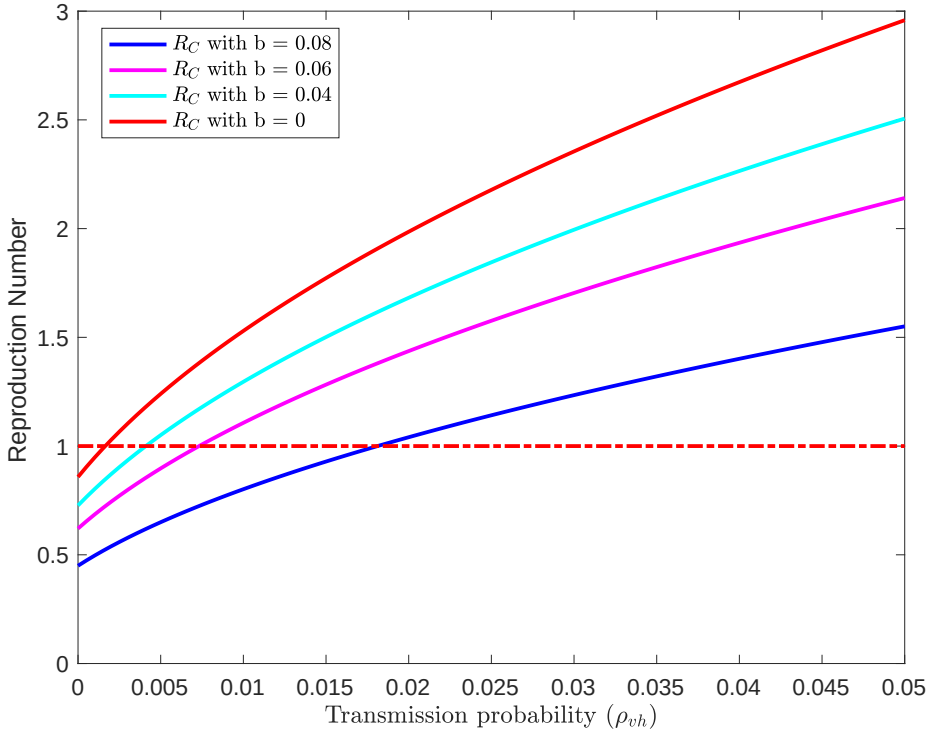

FIGURE 4. A plot of the control reproduction number for different values of the sterile release rate and the transmission probability from mosquitoes to humans.

A surface plot for the control reproduction number as a function of the sterile male mosquito release and the transmission probability from infectious humans to susceptible mosquitoes is delineated in Figure 5. In the absence of both treatment and vaccination, malaria persists in the population if the sterile male mosquito release rate is below 0.07 (that is, $b < 0.07$) as shown in Figure 5 (i). In the presence of treatment but without vaccination, Figure 5 (ii) suggests that malaria will persists if the sterile male mosquito release rate is below 0.04 (that is, $b < 0.04$). This can be attributed to the reduction in the number of infectious humans for susceptible mosquitoes to feed on due to malaria treatment in humans. In the presence of vaccination but without malaria treatment, the control reproduction number lies between 0.2 and 0.4 (that is, $0.2 < \mathcal{R}_C < 0.4$), but in the presence of both vaccination and malaria treatment, $\mathcal{R}_C < 0.3$ as shown in Figures 5 (iii) and (iv).

3.4.2. *Effect of Treatment, Vaccination and Male Mosquito Release.* We investigate the combined effects of malaria treatment in humans, vaccination and sterile mosquito release on the spread of malaria by generating a surface plot of $\mathcal{R}_C$ as a function of treatment and sterile release rate while altering the vaccination rate as shown in Figure 6. In the absence of vaccination ($\xi = 0$), the control reproduction number is above one when the male mosquito release rate is below 0.04 ($b < 0.04$) as shown in Figure 6 (i), and in the presence of vaccination, the control reproduction number as a function of b and u is below 0.37 as shown in Figure 6 (ii). This is attributed to the fact that vaccination and malaria

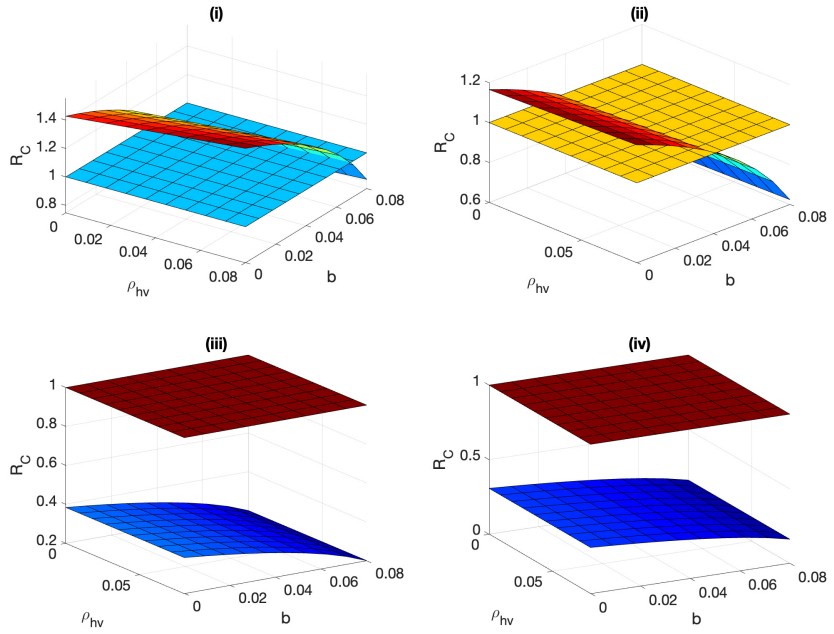

FIGURE 5. Surface plots of the control reproduction number as a function of the transmission probability from infectious humans to susceptible mosquitoes and the sterile male mosquito release rate, when (i) $u = 0$ and $\xi = 0$, (ii) $u > 0$ and $\xi = 0$, (iii) $\xi > 0$ and $u = 0$, (iv) $u > 0$ and $\xi > 0$.

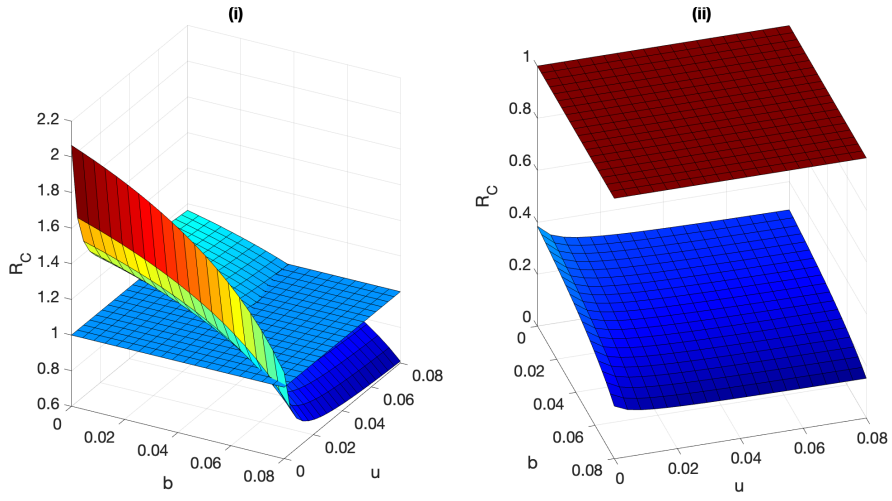

FIGURE 6. Surface plots of the control reproduction number as a function of the rate of malaria treatment in humans and the sterile male mosquito release rate, when (i) $\xi = 0$, (ii) $\xi > 0$.

treatment lower the parasite reservoir thereby increasing the impact on mosquito reduction, and hence a reduction in malaria prevalence.

4. Optimal Control of Vaccination, Treatment, and Sterile Male Mosquito Release

Current strategies for malaria control in humans encompass the use of insecticide-treated bed nets, indoor residual spraying, antimalarial medications, and more recently, vaccines such as RTS,S/AS01 and R21/Matrix-M. Although these interventions have demonstrated efficacy in reducing malaria transmission, complete eradication of the disease remains challenging due to factors such as the emergence of drug-resistant parasites, insecticide-resistant mosquitoes, and logistical barriers. A promising integrated approach combines sterile insect technique (SIT) with traditional malaria control measures like treatment and vaccination. SIT involves the release of sterilized male mosquitoes into the environment, where they mate with females, leading to the production of non-viable offspring. This biological control strategy diminishes the mosquito population without causing harm to the surrounding ecosystem. When combined with antimalarial treatment and vaccination, this approach has the potential to generate synergistic effects in the management and potential elimination of malaria. We introduce optimal control in our model by assuming that the rate of malaria treatment (u), sterile male mosquito release rate (b) and the malaria vaccination rate in humans (ξ) are functions of time. That is, $u = u(t)$, $b = b(t)$ and $\xi = \xi(t)$. We define the objective functional $J(b, u, \xi)$ of our optimal control problem as

$$\begin{aligned} J(b,u,\xi) = &\int_0^T \left[A_1E_n(t) + A_2E_s(t) + A_3I_n(t) + A_4I_s(t) + A_5N_v(t))\right] dt \\ &+ \int_0^T \left[B_0\xi(t)(S_n(t) + S_s(t)) + B_1b(t)M(t) + B_2u(t)(I_n(t) + I_s(t))\right. \\ &\qquad \left. + C_1b^2(t) + C_2u^2(t) + C_3\xi^2(t)\right] dt, \end{aligned} \tag{4.1}$$

where the weight constants A_1, A_2, A_3, A_4, A_5, B_0, B_1, B_2, C_1, C_2, and C_3 are positive. In the objective functional, $\xi(t)(S_n(t) + S_s(t))$ is the number of humans vaccinated and B_0 is the cost per individual vaccinated. Thus, the term $B_0\xi(t)(S_n(t) + S_s(t)) + C_3\xi^2(t)$ represents the non-linear cost that arises from vaccination and difficulties faced when implementing a successful vaccination program. Similarly, $u(t)(I_n(t) + I_s(t))$ is the number of infectious humans treated and B_2 is the unit cost of treatment, so that the term $B_2u(t)(I_n(t) + I_s(t)) + C_2u^2(t)$ represents the non-linear cost associated with malaria treatment and the difficulties faced when implementing a successful treatment program. Finally, $b(t)M(t)$ is the number of sterile male mosquitoes introduced and B_1 is the cost of introducing a single sterile male mosquito, so that the term $B_1b(t)M(t) + C_1b^2(t)$ represents a non-linear cost associated with sterile male mosquito release. Thus, our optimal control problem is to find a control triple $(b, u, \xi) \in \mathcal{U}$ such that

$$J(b^*, u^*, \xi^*) = \min_{(b,u,\xi)\in\mathcal{U}} J(b, u, \xi)$$

subject to the state system for humans

$$\begin{aligned} \frac{dS_n}{dt} &= p\Lambda_h + \sigma\mathbf{u}(\mathbf{t})I_n - \lambda_nS_n - (\mu_h + \xi(\mathbf{t}))S_n, \\ \frac{dE_n}{dt} &= \lambda_nS_n - (\psi_n + \mu_h)E_n, \\ \frac{dI_n}{dt} &= \psi_nE_n - (\delta_n + \gamma_n + \mu_h + \mathbf{u}(\mathbf{t}))I_n, \\ \frac{dS_s}{dt} &= (1-p)\Lambda_h + \sigma\mathbf{u}(\mathbf{t})I_s + \theta R_s - \lambda_sS_s - (\mu_h + \xi(\mathbf{t}))S_s, \end{aligned} \tag{4.2}$$

$$\begin{aligned}
\frac{dE_s}{dt} &= \lambda_s S_s + (1-\varepsilon)\lambda_s V - (\psi_s + \mu_h)E_s,\\
\frac{dI_s}{dt} &= \psi_s E_s - (\delta_s + \gamma_s + \mu_h + \mathbf{u(t)})I_s,\\
\frac{dV}{dt} &= \xi(\mathbf{t})(S_n + S_s) - (1-\varepsilon)\lambda_s V - \mu_h V,\\
\frac{dR_s}{dt} &= (\gamma_n + (1-\sigma)\mathbf{u(t)})I_n + (\gamma_s + (1-\sigma)\mathbf{u(t)})I_s - (\theta + \mu_h)R_s,
\end{aligned}$$

and state system for both the fertile and sterile mosquitoes

$$\begin{aligned}
\frac{dS_v}{dt} &= \frac{aN_v}{N_v + M}N_v - \lambda_v S_v - (\mu_{1v} + \mu_{2v}(N_v + M))S_v,\\
\frac{dE_v}{dt} &= \lambda_v S_v - \alpha_v E_v - (\mu_{1v} + \mu_{2v}(N_v + M))E_v,\\
\frac{dI_v}{dt} &= \alpha_v E_v - (\mu_{1v} + \mu_{2v}(N_v + M))I_v,\\
\frac{dM}{dt} &= \mathbf{b(t)}N_v - (\mu_{1v} + \mu_{2v}(N_v + M))M,
\end{aligned} \tag{4.3}$$

where the set of all admissible controls is

$$\mathcal{U} = \left\{ (b,u,\xi) \in (L^\infty(0,T))^3 \middle| 0 \le b(t) \le b_{\max}, 0 \le u(t) \le u_{\max}, 0 \le \xi(t) \le \xi_{\max} \right\}.$$

In the case where $b = 0$, no sterile male mosquitoes are released, and $b = b_{\max}$ represents the highest possible rate of sterile mosquito release. Similarly, $u = 0$ shows the absence of malaria treatment for humans, while $u = u_{\max}$ indicates the maximum rate of malaria treatment for humans. Lastly, $\xi = 0$ represents the case where no susceptible humans receive the malaria vaccine, while $\xi = \xi_{\max}$ delineates the maximum vaccination rate.

Theorem 4.1. *There exists an optimal control triple $(b^*, u^*, \xi^*) \in \mathcal{U}$ which minimizes the objective functional J subject to the state system (4.2) - (4.3).*

Proof. Follows as in Mohammed-Awel and Numfor [30, 34]. □

We characterize the control triple by using the Pontryagin's Minimum Principle [36]. To do this, we introduce adjoint functions λ_j, $j = 1, 2, \cdots, 12$, and append the integrand of the objective functional in equation (4.1) to the right-hand side of the state system (4.2) - (4.3). To characterize the optimal control triple, we construct the Hamiltonian $H = H(S_n, E_n, I_n, S_s, E_s, I_s, V, R_s, S_v, E_v, I_v, M, \lambda_1, \lambda_2, \lambda_3, \cdots, \lambda_{12})$, where

$$\begin{aligned}
H &= A_1E_n + A_2E_S + A_3I_n + A_4I_s + A_5N_v + B_0\xi(S_n + S_s) + B_1bM + B_2u(I_n + I_s)\\
&\quad + C_1b^2 + C_2u^2 + C_3\xi^2 + \lambda_1\dot{S}_n + \lambda_2\dot{E}_n + \lambda_3\dot{I}_n + \lambda_4\dot{S}_s + \lambda_5\dot{E}_s + \lambda_6\dot{I}_s + \lambda_7\dot{V}\\
&\quad + \lambda_8\dot{R}_s + \lambda_9\dot{S}_v + \lambda_{10}\dot{E}_v + \lambda_{11}\dot{I}_v + \lambda_{12}\dot{M},
\end{aligned}$$

where $\dot{M}$ denotes the rate of change of M with respect to time t.

Theorem 4.2. *Given optimal controls b^*, u^* and ξ^* with corresponding states S_n^*, E_n^*, I_n^*, S_s^*, E_s^*, I_s^*, V^*, R_s^*, S_v^*, E_v^*, I_v^*, and M^*, there exist adjoint functions λ_j, $j = 1, 2, \cdots, 12$ satisfying equations*

(4.2) - (4.3). *Furthermore, the optimal controls are characterized as*

$$\begin{aligned}
b^*(t) &= \min\left\{b_{max}, \max\left\{0, -\frac{B_1 M + N_v\lambda_{12}}{2C_1}\right\}\right\},\\
u^*(t) &= \min\left\{u_{max}, \max\left\{0, \frac{-B_2(I_n+I_s) - \sigma I_n\lambda_1 + I_n\lambda_3 - \sigma I_s\lambda_4 + I_s\lambda_6 - ((1-\sigma)I_n + (1-\sigma)I_s)\lambda_8}{2C_2}\right\}\right\},\\
\xi^*(t) &= \min\left\{u_{max}, \max\left\{0, \frac{S_n\lambda_1 + S_s\lambda_4 - B_1(S_n+S_s)}{2C_3}\right\}\right\}. \qquad (4.4)
\end{aligned}$$

Proof. We derive the adjoint system by taking the partial derivative of the Hamiltonian with respect to each of the state functions. That is,

$$\frac{d\lambda_1}{dt} = -\frac{\partial H}{\partial S_n}, \qquad \frac{d\lambda_2}{dt} = -\frac{\partial H}{\partial E_n}, \qquad \frac{d\lambda_3}{dt} = -\frac{\partial H}{\partial I_n}, \quad \cdots, \quad \frac{d\lambda_{12}}{dt} = -\frac{\partial H}{\partial M}. \qquad (4.5)$$

Using the relationship in equation (4.5), we obtain the following adjoint system:

$$\begin{aligned}
\frac{d\lambda_1}{dt} &= \left(\lambda_n + \mu_h + \xi - \frac{\lambda_n S_n}{N_h}\right)\lambda_1 + \left(\frac{S_n}{N_h} - 1\right)\lambda_n\lambda_2 - \frac{S_s\lambda_s}{N_h}\lambda_4 + (S_s + (1-\varepsilon)V)\frac{\lambda_s}{N_h}\lambda\\
&\quad - \left(\xi + \frac{(1-\varepsilon)V\lambda_s}{N_h}\right)\lambda_7 + \frac{\lambda_v S_v}{N_h}(\lambda_{10} - \lambda_9) - B_0\xi,\\
\frac{d\lambda_2}{dt} &= -\frac{\lambda_n S_n}{N_h}\lambda_1 + \left(\frac{\lambda_n S_n}{N_h} + \psi_n + \mu_h\right)\lambda_2 - \psi_n\lambda_3 - \frac{\lambda_s S_s}{N_h}\lambda_4 + (S_s + (1-\varepsilon)V)\frac{\lambda_s}{N_h}\lambda_5\\
&\quad - \frac{(1-\varepsilon)V\lambda_s}{N_h}\lambda_7 + \frac{\lambda_v S_v}{N_h}(\lambda_{10} - \lambda_9) - A_1,\\
\frac{d\lambda_3}{dt} &= -\left(\sigma u + \frac{\lambda_n S_n}{N_h}\right)\lambda_1 + \frac{\lambda_n S_n}{N_h}\lambda_2 + K_1\lambda_3 - \frac{\lambda_s S_s}{N_h}\lambda_4 + (S_s + (1-\varepsilon)V)\frac{\lambda_s}{N_h}\lambda_5\\
&\quad - \frac{(1-\varepsilon)V\lambda_s}{N_h}\lambda_7 - K_3\lambda_8 + \left(\frac{\lambda_v}{N_h} - \frac{\rho_{hv}}{N_h}\right)S_v(\lambda_{10} - \lambda_9) - B_2 u - A_3,\\
\frac{d\lambda_4}{dt} &= \frac{\lambda_n S_n}{N_h}(\lambda_2 - \lambda_1) + \left(\lambda_s + \mu_h + \xi - \frac{\lambda_s S_s}{Nh}\right)\lambda_4 + \left(\frac{S_s}{N_h} - 1 + \frac{(1-\varepsilon)V}{N_h}\right)\lambda_s\lambda_5\\
&\quad - \left(\xi + \frac{(1-\varepsilon)V\lambda_s}{N_h}\right)\lambda_7 + \frac{\lambda_v S_v}{N_h}(\lambda_{10} - \lambda_9) - B_0\xi,\\
\frac{d\lambda_5}{dt} &= \frac{\lambda_n S_n}{N_h}(\lambda_2 - \lambda_1) - \frac{\lambda_s S_s}{Nh}\lambda_4 + \left(\psi_s + \mu_h + (S_s + (1-\varepsilon)V)\frac{\lambda_s}{N_h}\right)\lambda_5 - \psi_s\lambda_6\\
&\quad - \frac{(1-\varepsilon)V\lambda_s}{N_h}\lambda_7 + \frac{\lambda_v S_v}{N_h}(\lambda_{10} - \lambda_9) - A_2,\\
\frac{d\lambda_6}{dt} &= \frac{\lambda_n S_n}{N_h}(\lambda_2 - \lambda_1) - \left(\sigma u + \frac{\lambda_s S_s}{N_h}\right)\lambda_4 + (S_s + (1-\varepsilon)V)\frac{\lambda_s}{N_h}\lambda_5\\
&\quad + K_2\lambda_6 - \frac{(1-\varepsilon)V\lambda_s}{N_h}\lambda_7 - K_4\lambda_8 + \left(\frac{\lambda_v}{N_h} - \frac{\tilde{\rho}_{hv}}{N_h}\right)S_v(\lambda_{10} - \lambda_9) - B_2 u - A_4,\\
\frac{d\lambda_7}{dt} &= \frac{\lambda_n S_n}{N_h}(\lambda_2 - \lambda_1) - \frac{\lambda_s S_s}{N_h}\lambda_4 + \left(\frac{S_s + (1-\varepsilon)V}{N_h} - (1-\varepsilon)\right)\lambda_s\lambda_5\\
&\quad + \left(\mu_h + (1-\varepsilon)\lambda_s\left[1 - \frac{V}{N_h}\right]\right)\lambda_7 + \frac{\lambda_v S_v}{N_h}(\lambda_{10} - \lambda_9), \qquad (4.6)
\end{aligned}$$

$$
\begin{aligned}
\frac{d\lambda_8}{dt} &= \frac{\lambda_n S_n}{N_h}(\lambda_2-\lambda_1)-\left(\theta+\frac{\lambda_s S_s}{N_h}\right)\lambda_4+(S_s+(1-\varepsilon)V)\frac{\lambda_s}{N_h}\lambda_5-\frac{(1-\varepsilon)V\lambda_s}{N_h}\lambda_7\\
&\quad +(\theta+\mu_h)\lambda_8+\left(\frac{\lambda_v}{N_h}-\frac{\hat{\rho}_{hv}}{N_h}\right)S_v(\lambda_{10}-\lambda_9),\\
\frac{d\lambda_9}{dt} &= (\lambda_v+\mu_v(N_v,M)+\mu_{2v}S_v-\left(\frac{aN_v^2+2aN_vM}{(N_v+M)^2}\right))\lambda_9+(\mu_{2v}E_v-\lambda_v)\lambda_{10}+\mu_{2v}I_v\lambda_{11}\\
&\quad +(\mu_{2v}M-b)\lambda_{12}-A_5,\\
\frac{d\lambda_{10}}{dt} &= (\mu_{2v}S_v-\left(\frac{aN_v^2+2aN_vM}{(N_v+M)^2}\right))\lambda_9+(\alpha_v+\mu_v(N_v,M)+\mu_{2v}E_v)\lambda_{10}\\
&\quad +(\mu_{2v}I_v-\alpha_v)\lambda_{11}+(\mu_{2v}M-b)\lambda_{12}-A_5,\\
\frac{d\lambda_{11}}{dt} &= \frac{\rho_{vh}S_n}{N_h}(\lambda_1-\lambda_2)+\frac{\tilde{\rho}_{vh}S_s}{N_h}\lambda_4-(S_s+(1-\varepsilon)V)\frac{\tilde{\rho}_{vh}}{N_h}\lambda_5+\frac{(1-\varepsilon)V\tilde{\rho}_{vh}}{N_h}\lambda_7+\mu_{2v}E_v\lambda_{10}\\
&\quad +(\mu_{2v}S_v-\left(\frac{aN_v^2+2aN_vM}{(N_v+M)^2}\right))\lambda_9+(\mu_v(N_v,M)+\mu_{2v}I_v)\lambda_{11}+(\mu_{2v}M-b)\lambda_{12}-A_5,\\
\frac{d\lambda_{12}}{dt} &= \left(\frac{aN_v^2}{(N_v+M)^2}+\mu_{2v}S_v\right)\lambda_9+\mu_{2v}E_v\lambda_{10}+\mu_{2v}I_v\lambda_{11}+(\mu_v(N_v,M)+\mu_{2v}M)\lambda_{12}-B_1b,
\end{aligned}
$$

with transversality conditions

$$\lambda_1(T)=\lambda_2(T)=\lambda_3(T)=\lambda_4(T)=\cdots=\lambda_{12}(T)=0.$$

To characterize the optimal control triple $(b,u,\xi)\in\mathcal{U}$, the partial derivatives of the Hamiltonian H with respect to each control are computed. This process yields the following:

$$
\begin{aligned}
\frac{\partial H}{\partial b} &= 2C_1b+B_1M+N_v\lambda_{12},\\
\frac{\partial H}{\partial u} &= B_2(I_n+I_s)+2C_2u+\sigma I_n\lambda_1-I_n\lambda_3+\sigma I_s\lambda_4-I_s\lambda_6+((1-\sigma)I_n+(1-\sigma)I_s)\lambda_8,\\
\frac{\partial H}{\partial \xi} &= B_0(S_n+S_s)+2C_3\xi-S_n\lambda_1-S_s\lambda_4.
\end{aligned}
$$

In the interior of the control set $\mathcal{U}$, we set $\frac{\partial H}{\partial b}=\frac{\partial H}{\partial u}=\frac{\partial H}{\partial \xi}=0$. Since our controls are bounded and the second derivatives satisfy $\frac{\partial^2 H}{\partial b^2}=2C_1>0$, $\frac{\partial^2 H}{\partial u^2}=2C_2>0$ and $\frac{\partial^2 H}{\partial \xi^2}=2C_3>0$, we obtain the optimal control characterization in equation (4.4). □

4.1. **Numerical Simulations.** We determine some of the values of the weight constants from the literature and use the parameter values in Table 1 to approximate the solutions of the optimality system. In the Unicef fact sheet on malaria vaccine [40], it is estimated that the cost per person per dose of the vaccine RTS,S/AS01 is €9.30 (approximately $9.76) and $3.90 per dose of R21/MatrixM. Thus, we set the unit cost of vaccinating non-immune and semi-immune susceptible humans to $B_1=6.83$. Additionally, in the Unicef fact sheet on malaria treatment [41], it is estimated that the cost per person of malaria treatment is between $0.65 and $96.90, depending on the type of medication. Therefore, we set the unit cost of treating non-immune and semi-immune infectious humans to $B_2=48.78$. Finally, the cost associated with the introduction of sterile male mosquitoes into a particular population through the Sterile Insect Technique (SIT) is contingent upon the size of the initiative, typically averaging at $110.12 for every 10,000 sterile male mosquitoes released [9]. Thus, we set $B_1=110.12/10000\approx 0.011$, and summarize the values of the weight constants in Table 2

Table 2: Weight constants of the objective functional (4.1).

Weight constant	A_1	A_2	A_3	A_4	A_5	B_0	B_1	B_2	C_1	C_2	C_3
Value	1	1	1	1	1	6.83	0.011	48.78	10	10	10

Using the Forward-Backward Sweep Method [25], the parameter values in Table 1 and the weight constants in Table 2, we explore different intervention strategies. For our numerical simulations, we use the initial condition $S_n(0) = 500$, $S_s(0) = 200$, $E_n(0) = E_s(0) = 0$, $I_n(0) = 30$, $I_s(0) = 15$, $V(0) = 0$, $R_s(0) = 0$, $S_v(0) = 5000$, $E_v(0) = 0$, $I_v(0) = 300$, and $M(0) = 5$ to investigate the following optimal control strategies:

(A) Optimal vaccination in the absence of malaria treatment and sterile male mosquito release (i.e. $\xi(t) > 0$, $b(t) = 0$ & $u(t) = 0$).
(B) Optimal treatment in the absence of sterile male mosquito release and vaccination (i.e. $u(t) > 0$, $b(t) = 0$ & $\xi(t) = 0$).
(C) Optimal sterile mosquito release in the absence of treatment and vaccination (i.e. $b(t) > 0$, $u(t) = 0$ & $\xi(t) = 0$).
(D) A combination of optimal malaria treatment and the sterile male mosquitoes in the absence of vaccination (i.e. $u(t) > 0, b(t) > 0$ & $\xi(t) = 0$).
(E) A combination of optimal vaccination and the release of sterile male mosquitoes but in the absence of malaria treatment (i.e. $b(t) > 0, \xi(t) > 0$ & $u(t) = 0$).
(F) A combination of optimal malaria treatment and vaccination in the absence of sterile male mosquito release (i.e. $u(t) > 0, \xi(t) > 0$ & $b(t) = 0$).
(G) A combination of optimal malaria treatment, vaccination and the release of sterile male mosquito release (i.e. $u(t) > 0, b(t) > 0$ & $\xi(t) > 0$).

4.1.1. *Optimal Vaccination in the Absence of Malaria Treatment and Sterile Male Mosquito Release.* Strategy A depicts the optimal effect of implementing vaccination-only in the population. Figure 7 (i) suggests a 66.59% decrease in the peak of prevalence for non-immune infectious individuals and 75.85% decrease in the number of semi-immune infectious humans at the end of the control period as shown in Figure 7 (ii). As depicted in Figure 7 (iii), the mosquito population experiences a 59.32% decrease in prevalence at the end of the control period. The control profile in Figure 7 (vi) suggests a maximum vaccination for a short period, followed by a decrease and a slight increase for the remainder of the control period, except for a few days prior to the end of the control.

4.1.2. *Optimal Treatment in the Absence of Sterile Male Mosquito Release and Vaccination.* Strategy B depicts the optimal effect of implementing treatment-only in the human population. Figure 8 (i) suggests a 48.27% decrease in the peak of prevalence for non-immune infectious individuals and a 77.69% decrease in the number of non-immune infectious individuals at the end of the control period. On the other hand, strategy B depicts a 27.83% decrease in the peak of prevalence for semi-immune infectious individuals and a 31.39% decrease in the number of non-immune infectious individuals at the end of the control period. There is a 17.65% decrease in the peak of malaria prevalence in mosquitoes and a 39.46% decrease in the number of infectious mosquitoes at the end of the control period. The control profile depicts constant treatment at the maximum level for about 344 days followed by a decrease in treatment until day 348, and eventually no treatment is recommended for the remainder of the time period.

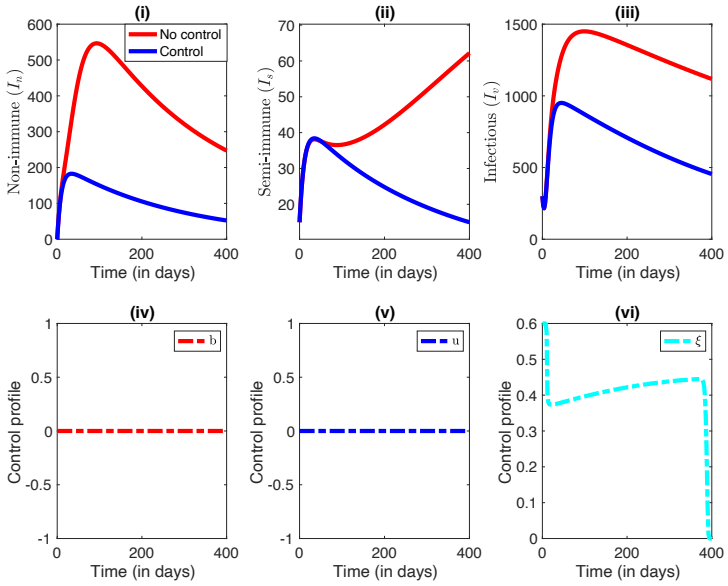

FIGURE 7. Simulations for the effect of optimal vaccination in the absence of malaria treatment and the sterile male mosquitoes when $b_{\max} = 0$, $u_{\max} = 0$ and $\xi_{\max} = 0.6$.

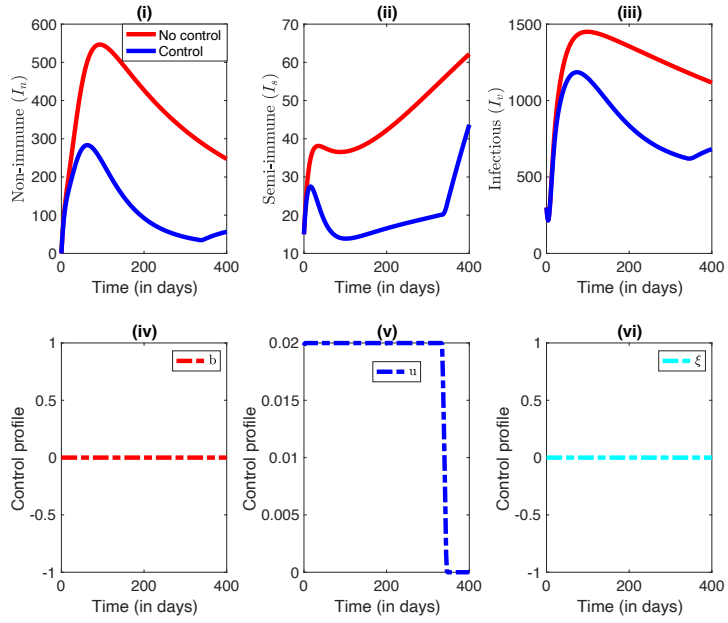

FIGURE 8. Simulations for the effect of optimal treatment in the absence of vaccination and the sterile male mosquitoes when $b_{\max} = 0$, $u_{\max} = 0.02$ and $\xi_{\max} = 0$.

4.1.3. *Optimal Sterile Mosquito Release in the Absence of Treatment and Vaccination.* The introduction of sterile male mosquito release in the absence of malaria treatment and vaccination (Strategy C)

suggests a minimal effect on malaria prevalence in humans, but with about 32.4% decrease in prevalence for the mosquito population throughout the entire time horizon as shown in Figure 9 (i) - (iii). The control profile indicates a maximum release of sterile male mosquitoes for about 326 days, followed by a decrease for the remainder of the time horizon.

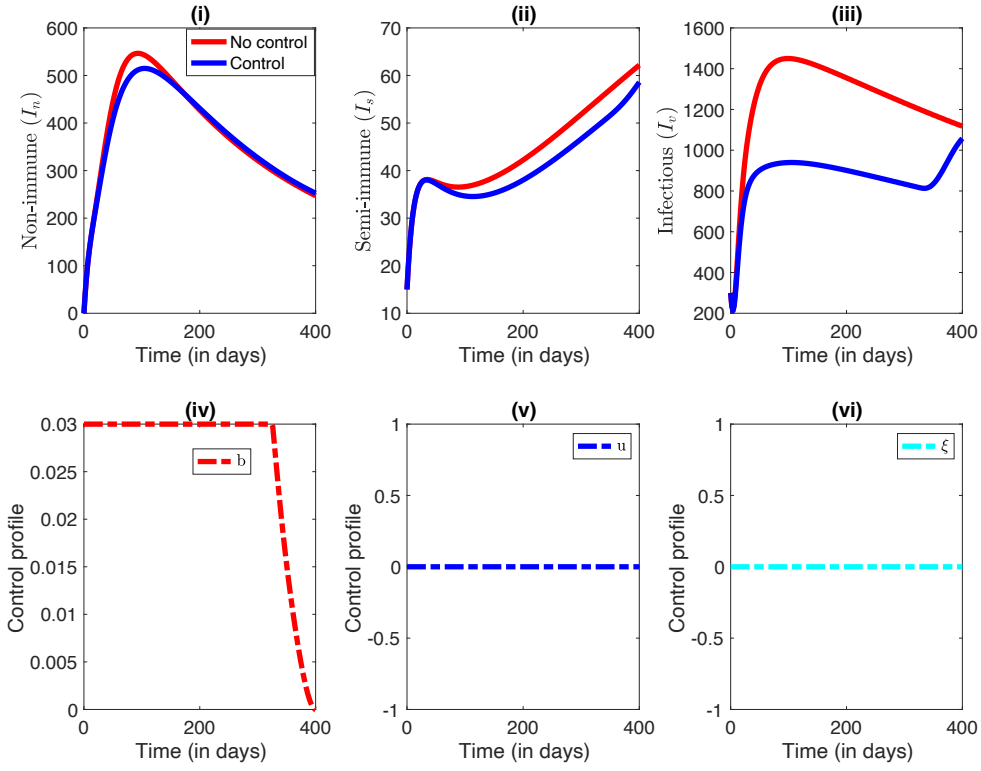

FIGURE 9. Simulations for the effect of optimal sterile male mosquito release in the absence of malaria treatment and vaccination when $b_{\max} = 0.03$, $u_{\max} = 0$ and $\xi_{\max} = 0$.

4.1.4. *Combined Effect of Optimal Malaria Treatment and Sterile Male Mosquito Release in the Absence of Vaccination.* Figure 10 depicts the combined effect of treatment and sterile male mosquito release. In Figure 10 (i), there a 54.21% decrease in the peak of non-immune infectious humans and a 72.48% decrease in the number of semi-immune infectious humans at the end of the control period. Moreover, there is a 68.24% decrease in malaria prevalence $(I_n + I_s)$ in humans. In the mosquito population, there is 51.85% decrease in malaria prevalence in the mosquito population. The control profiles suggest that malaria treatment should be administered at the maximum level for 334 days, followed by a decrease until day 348 as shown in Figure 10 (v), but sterile male mosquitoes should be released for 322 days at the maximum level followed by a decrease afterwards as represented in Figure 10 (iv).

4.1.5. *Combined Effect of Optimal Malaria Vaccination and Sterile Male Mosquito Release in the Absence of Malaria Treatment.* Simulations of the model in the presence of sterile male mosquito release and malaria vaccination are depicted in Figure 11. In Figure 11 (i), there is 66.68% decrease in the peak

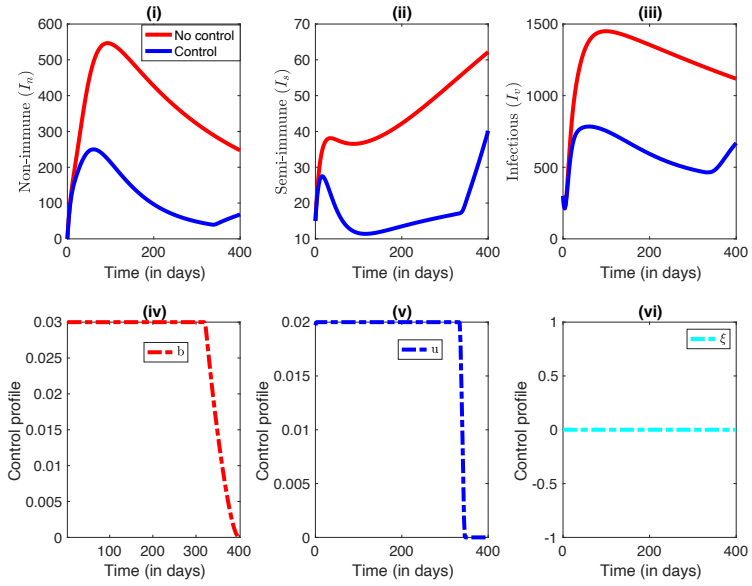

FIGURE 10. Simulations for the combined effect of optimal malaria treatment and the sterile male mosquitoes in the absence of vaccination when $b_{\max} = 0.03$, $u_{\max} = 0.02$ and $\xi_{\max} = 0$.

of non-immune infectious humans when sterile mosquitoes and malaria vaccine are applied compared to the case in the absence of any form of control.

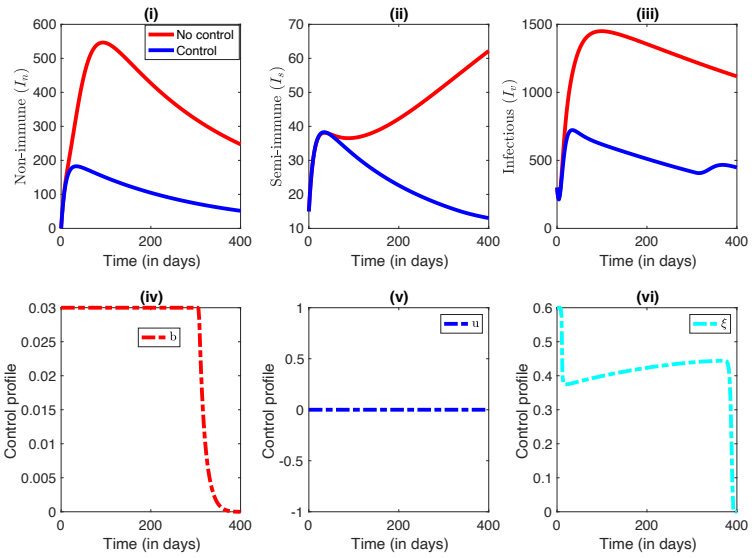

FIGURE 11. Simulations for the combined effect of optimal vaccination and sterile male mosquitoes, but in the absence of treatment when $b_{\max} = 0.03$, $\xi_{\max} = 0.6$ and $u_{\max} = 0$.

On the other hand, there is a 79.01% decrease in the number of infectious semi-immune humans at the end of the control period in the presence of both forms of control relative to the absence of control. The infectious mosquitoes experience a 54.44% decrease in the presence of both controls as represented in Figure 11 (iii). The control profiles suggest the release of sterile male mosquitoes at the maximum level for 306 days, followed by a decrease for the remainder of the control period.

4.1.6. *Combined Effect of Optimal Malaria Vaccination and Malaria Treatment in the Absence of Sterile Male Mosquito Release.* Figure 12 delineates the effect of pharmaceutical interventions where malaria treatment and vaccination are administered but in the absence of the sterile male mosquito release. With vaccination and treatment, simulations portray a 93.37% decrease in malaria prevalence in humans $(I_n + I_s)$ and a 78.85% decrease in malaria prevalence in the mosquito population. Additionally, there is a 75.91% decrease in the peak of prevalence of the non-immune infectious humans. The vaccination and treatment profiles suggest an optimal treatment for about 164 days, followed by a decrease until day 348, and maximum vaccination for about 44 days, followed by a decrease between days 45 and 382 as shown in Figure 12 (vi).

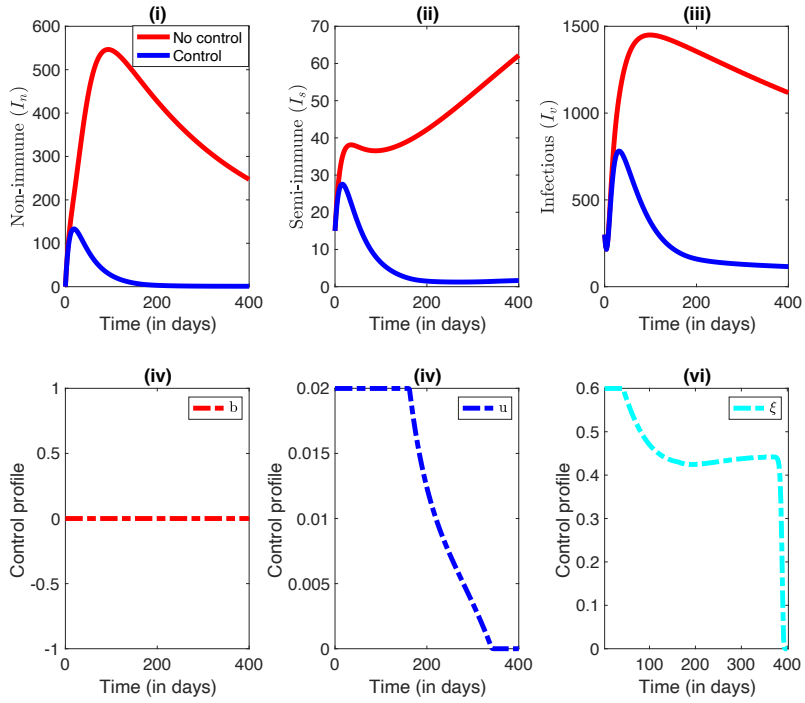

FIGURE 12. Simulations for the combined effect of optimal malaria treatment and vaccination, but in the absence of sterile male mosquitoes when $u_{\max} = 0.02$, $\xi_{\max} = 0.6$ and $b_{\max} = 0$.

4.1.7. *Combined Effect of Optimal Malaria Vaccination, Malaria Treatment, and Sterile Male Mosquito Release.* The results of simulations for strategy G (malaria treatment, vaccination and sterile male mosquito release) are represented in Figure 13. In the presence of all three forms of control, there is an 93.45% decrease in malaria prevalence humans $(I_n + I_s)$, and approximately a 75.86% decrease in the

peak of malaria prevalence in the non-immune infectious class. In the infectious mosquito population, there is 83.01% decrease in malaria prevalence and a 89.81% decrease in the peak of prevalence. The application of all three forms of controls suggest that sterile male mosquitoes should be released at the maximum level for 306 days followed by a decrease afterwards, but malaria treatment should be administered at the maximum level for 154 days, followed by a decrease. The vaccination program suggests a maximum vaccination about 42 days, followed by a decrease between days 43 and 376 as shown in Figure 12 (iv) - (vi).

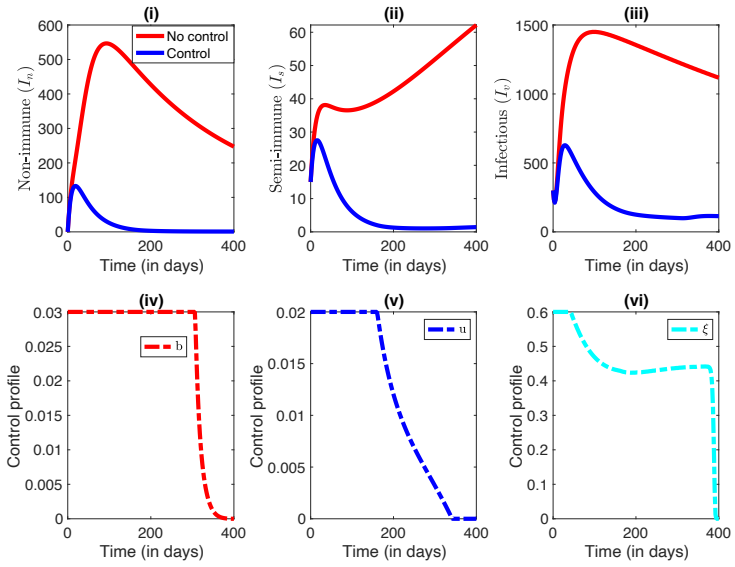

FIGURE 13. Simulations for the combined effect of optimal malaria treatment, vaccination, and the sterile male mosquitoes when $b_{\max} = 0.03$, $u_{\max} = 0.02$, and $\xi_{\max} = 0.6$.

The results in Figures 10 - 13 suggest that there is a synergy between the interventions, such that sterile release technique reduces the number of infected mosquitoes, enhancing the effectiveness of vaccines and treatments. Moreover, vaccination and treatment lower the parasite reservoir, thereby increasing the impact of mosquito population reduction.

5. Cost-effectiveness Analysis

Cost-effectiveness analysis is a crucial tool for optimizing resource allocation in disease control and ecological management. By integrating mathematical models with economic principles, cost-effectiveness analysis helps policymakers choose interventions that maximize health benefits while minimizing costs, ensuring sustainable and effective decision-making. Some key metrics in cost-effectiveness analysis are the infection averted ratio (IAR) and the incremental cost-effectiveness ratio (ICER). The IAR is a measure used to assess the effectiveness of an intervention in reducing the number of infections. It represents the proportion of infections prevented due to the intervention. A higher IAR value indicates a more effective intervention in controlling disease spread. The infection averted ratio is computed as [7]

$$\text{IAR} = \frac{\text{Number of infections averted}}{\text{Number of recovered}},$$

where the number of infections averted is the difference between the total infected individuals without control and the total infected individuals with control. The IAR for strategies $A-G$ are displayed in Table 3 in an increasing order of effectiveness, based on infection averted ratio.

Table 3: Total infections and infection averted ratios.

Strategy	Total infections averted	Total cost	IAR
C: $b>0$, $u=0$, $\xi=0$	3.931×10^3	3.0823×10^6	0.2409
B: $u>0$, $b=0$, $\xi=0$	1.1031×10^5	5.2021×10^4	0.5383
D: $b>0$, $u>0$, $\xi=0$	1.1329×10^5	3.1091×10^6	0.5891
A: $\xi>0$, $b=0$, $u=0$	5.3251×10^4	3.8866×10^3	0.6141
E: $b>0$, $\xi>0$, $u=0$	5.8908×10^4	3.1944×10^6	0.7101
F: $u>0$, $\xi>0$, $b=0$	1.344×10^5	3.8388×10^4	0.9487
G: $b>0$, $u>0$, $\xi>0$	1.3913×10^5	3.1948×10^6	1.0732

In Table 3, the total cost is obtained from

$$\text{Cost}=\int_0^T [B_0\xi(t)(S_n(t)+S_s(t))+B_1b(t)M(t)+B_2u(t)(I_n(t)+I_s(t))+C_1b^2(t)+C_2u^2(t)+C_3\xi^2(t)]dt.$$

This cost will be used in the computation of the incremental cost-effectiveness ratio. A bar graph representation for the IAR is represented in Figure 14.

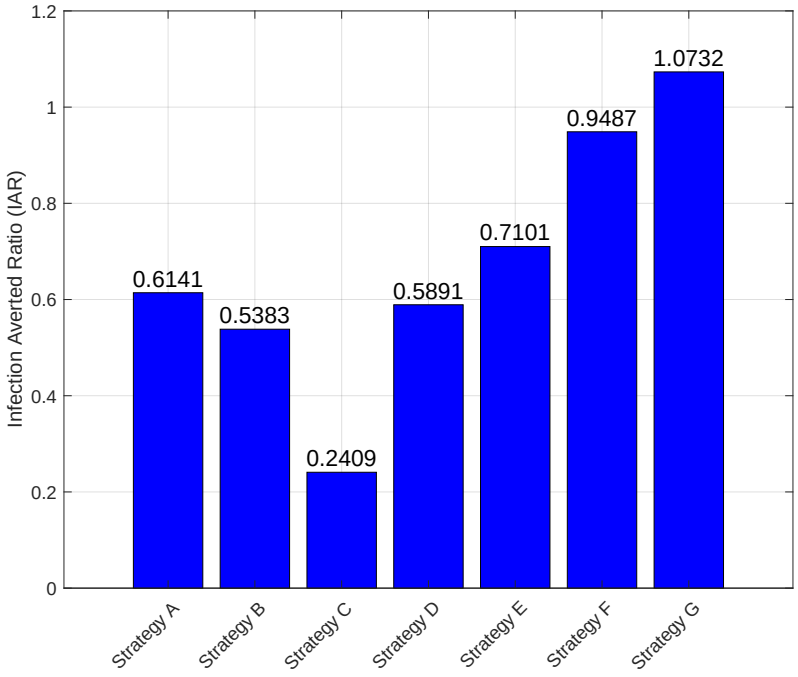

FIGURE 14. Infection averted ratios for strategies A - G.

Figure 14 suggests that strategy G, which consists of all three controls, is the best strategy at averting infections, followed strategy F (treatment and vaccination, but in the absence of sterile male mosquito release), and strategy C is the least at averting infections. Strategy C consists of releasing sterile male mosquitoes in the absence of treatment and vaccination. We consider the ICER which compares the cost and effectiveness of two competing strategies. Using the total number of averted infections in Table 14, we compute the ICER as the difference between the total number of infected individuals without control and those with control, determined within the entire time horizon [1, 7, 8, 20, 21, 24]. That is,

$$\text{ICER} = \frac{\text{Difference in total costs by strategies } i \text{ and } j}{\text{Difference in total cost of averted infections by strategies } i \text{ and } j}.$$

A lower ICER indicates a more cost-effective intervention and higher ICER signifies that the intervention is relatively expensive compared to the health benefits it provides. Starting with the strategy with the smallest IAR, the ICER for strategies B (Malaria treatment in the absence of sterile male mosquito release and vaccination) and C (sterile male mosquito release in the absence of treatment and vaccination) are computed as follows:

$$\begin{aligned} \text{ICER(C)} &= \frac{3.0823 \times 10^6}{3.931 \times 10^3} = 748.101, \\ \text{ICER(B)} &= \frac{5.2021 \times 10^4 - 3.0823 \times 10^6}{1.1031 \times 10^5 - 3.931 \times 10^3} = -28.4857. \end{aligned}$$

Since ICER(C) > ICER(B), it follows that strategy C is more costly and less effective that strategy B. Thus, strategy C is removed from further analysis, based on the ICER computation. Next, we compare strategies B and D, where strategy D consists of sterile male mosquito release and treatment, but in the absence of malaria treatment. Now,

$$\begin{aligned} \text{ICER(B)} &= \frac{5.2021 \times 10^4}{1.1031 \times 10^5} = 0.471589, \\ \text{ICER(D)} &= \frac{3.1091 \times 10^6 - 5.2021 \times 10^4}{1.1329 \times 10^5 - 1.1031 \times 10^5} = 1024.89. \end{aligned}$$

The value of ICER(D) is greater than than of ICER(B). Thus, based on ICER computation, strategy D is more costly and less effective than strategy B. Consequently, we eliminate strategy D from further consideration, and compare strategies B and A, where strategy A consists of malaria vaccination in the absence of sterile male mosquito release and treatment. Computing the ICER for strategies A and B, we obtain

$$\begin{aligned} \text{ICER(B)} &= \frac{5.2021 \times 10^4}{1.1031 \times 10^5} = 0.471589, \\ \text{ICER(A)} &= \frac{3.8866 \times 10^3 - 5.2021 \times 10^4}{5.3251 \times 10^4 - 1.1031 \times 10^5} = 0.84359. \end{aligned}$$

The value of ICER(A) is greater than than of ICER(B). Thus, based on ICER computation, strategy A is more costly and less effective that strategy B. Consequently, we eliminate strategy A from further consideration, and compare strategies B and E, where strategy E consists of a combination of sterile male mosquito release and vaccination, but in the absence of malaria treatment. Computing the ICER for strategies B and E, we obtain

$$\begin{aligned}\text{ICER(B)} &= \frac{5.2021\times10^4}{1.1031\times10^5} = 0.471589,\\ \text{ICER(E)} &= \frac{3.1944\times10^6 - 5.2021\times10^4}{5.8908\times10^4 - 1.1031\times10^5} = -61.1334.\end{aligned}$$

The value of ICER(B) is greater than than of ICER(E). Thus, based on ICER computation, strategy B is more costly and less effective that strategy E. Consequently, we eliminate strategy B from further consideration, and compare strategies E and F, where strategy F consists of a combination of malaria treatment and vaccination, but in the absence of sterile male mosquito release. Computing the ICER for strategies E and F, we obtain

$$\begin{aligned}\text{ICER(E)} &= \frac{3.1944\times10^6}{5.8908\times10^4} = 54.2269,\\ \text{ICER(F)} &= \frac{3.8388\times10^4 - 3.1944\times10^6}{1.344\times10^5 - 5.8908\times10^4} = -41.8059.\end{aligned}$$

The value of ICER(E) is greater than than of ICER(F). Thus, based on ICER computation, strategy E is more costly and less effective that strategy F. Consequently, we eliminate strategy E from further consideration, and compare strategies F and G, where strategy G consists of a combination of malaria treatment, sterile male mosquito release and vaccination. Computing the ICER for strategies F and G, we obtain

$$\begin{aligned}\text{ICER(F)} &= \frac{3.8388\times10^4}{1.344\times10^5} = 0.285625,\\ \text{ICER(G)} &= \frac{3.1948\times10^6 - 3.8388\times10^4}{1.3913\times10^5 - 1.344\times10^5} = 667.318.\end{aligned}$$

We observe from the ICER computation that ICER(G) is greater than than of ICER(F). Thus, based on the ICER computation, we conclude that strategy F (vaccination and treatment in the absence of sterile male mosquito release) is the most cost-effective in reducing malaria cases in humans, followed by strategy G (all three controls). On the other hand, strategy C (sterile male mosquito release in the absence of treatment and vaccination) is the least cost-effective strategy at reducing the number of malaria cases in humans.

6. Conclusion

In this study, we developed and analyzed a mathematical model to investigate the effects of treatment, vaccination, and sterile male mosquito release on malaria transmission. The model incorporates different levels of human immunity, distinguishing between non-immune and semi-immune populations to better capture the dynamics of malaria spread and control. Our results provide important insights into the effectiveness of various intervention strategies in reducing malaria prevalence in both human and mosquito populations.

We determined the control reproduction number, using the next-generation method and established the local asymptotic stability of the disease-free equilibrium when $\mathcal{R}_C < 1$. This stability condition implies that malaria can be eliminated from the population if effective intervention strategies are implemented to maintain $\mathcal{R}_C$ below unity. By generating a plot of the control reproduction number $\mathcal{R}_C$ as a function of the transmission probability from infectious mosquitoes to non-immune susceptible humans (ρ_{vh}) but at different levels of sterile male mosquito release rate (b) as shown in Figure 4, we observed significant variations in malaria transmission dynamics. As the sterile release rate increases,

the control reproduction number decreases, and it requires a higher transmission rate for malaria to persist in the population. This highlights the importance of sterile male mosquitoes in curbing the spread of malaria in the population. A global sensitivity analysis with the reproduction number as the outcome variable was conducted to determine the key parameters influencing malaria transmission. Our analysis identified vaccination coverage, treatment efficacy, and the sterile mosquito release rate as some of the critical factors in controlling the spread of the disease. This highlights the necessity of a multi-faceted approach that combines pharmaceutical and vector-targeted interventions to effectively curb malaria transmission.

Furthermore, focusing on vaccination, treatment, and the sterile mosquito release rate, we formulated and analyzed an optimal control problem incorporating vaccination, treatment, and sterile male mosquito release as control functions. Our findings indicate that the simultaneous implementation of all three control strategies is the most effective in reducing malaria prevalence among both humans and mosquitoes. This underscores the importance of integrating multiple control measures to achieve maximum impact in malaria eradication efforts. A cost-effectiveness analysis was carried out to assess the economic feasibility of various intervention strategies. Based on the Infection Averted Ratio (IAR), the most cost-effective strategy was Strategy G, which combined treatment, vaccination, and sterile mosquito release. However, based on the Incremental Cost-Effectiveness Ratio (ICER), Strategy F, which comprises vaccination and treatment, but without sterile male mosquito release, emerged as the most cost-effective strategy for reducing malaria cases in humans, followed by strategy G. Strategy C, which relied solely on sterile mosquito release, was found to be the least cost-effective in reducing human malaria cases.

This research offers valuable insights into the complex dynamics of malaria transmission, emphasizing the importance of accounting for varying levels of immunity within human populations when developing effective control measures. The optimal control results suggest synergy between interventions whereby sterile insect technique (SIT) reduces the number of infected mosquitoes, enhancing the effectiveness of vaccines and treatments. Our findings suggest that a comprehensive intervention strategy that integrates treatment, vaccination, and sterile mosquito release is the most effective approach for reducing malaria transmission. However, from a cost-effectiveness perspective, prioritizing vaccination and treatment is the most feasible option in resource-limited settings.

References

[1] A. Abidemidemi, Fatmawati, O. J. Peter, *Deterministic Double Dose Vaccination Model of COVID-19 Transmission Dynamics - Optimal Control Strategies with Cost-Effectiveness Analysis*, Commun. Biomath. Sci. **7**(2024), 1-33.

[2] L. J. S. Allen, An Introduction to Mathematical Biology, *Pearson Education Hall Inc*, London, 2007.

[3] M. Y. Ali and I. A. Khan, *Computing Determinants of Block Matrices,* UITS J. Sci. & Eng. **7**(2020), 5-11.

[4] F. B. Agusto, E. Numfor, K. Srinivasan, E. A. Iboi, A. Fulk, J. M. S. Onge, and A. T. Peterson. *Impact of public sentiments on the transmission of COVID-19 across a geographical gradient*, Peer J **11**(2023): e14736.

[5] F. B. Agusto, A. B. Gumel, P. E. Parham, *Qualitative assessment of the role of temperature variations on malaria transmission dynamics,* J. Biol. Syst. **23**(2015): 1550030.

[6] F. B. Agusto, N. Marcus, and K. O Okosun, *Application of optimal control to the epidemiology of malaria,* Electron J. Differ. Equ. **2012**(2012), 1–22.

[7] F. B. Agusto and I.M. Elmojtaba, *Optimal control and cost-effective analysis of a malaria/visceral leishmaniasis co-infection,* PLoS ONE **12**(2017): e0171102. DOI:10.1371/journal.pone.0171102.

[8] V. P. Bajiya, S. Bugalia, J. P. Tripathi and M. Martcheva, *Deciphering thetransmission dynamics of COVID-19 in India: Optimal control and cost effective analysis,*. J. Biol. Dyn. **16**(2022), 665-712.

[9] A. Baly, A, R. Gato, Z. Garcia, M. Rodriguez and P. Van der Stuyft, *The cost of the production and release of male Aedes aegypti mosquitoes sterilised by irradiation,* Trop. Med. Int. Health **30**(2025): 210-8. https://doi.org/10.1111/tmi.14086.

[10] S. M. Blower and H. Dowlatabadi, *Sensitivity and uncertainty analysis of complex models of disease transmission: an hiv model, as an example,* Int. Stat. Rev. **62**(1994), 229-243.
[11] L. Cai, L. Bao, L. Rose, J. Summers and W. Ding, *Malaria modeling and optimal control using sterile insect technique and insecticide-treated nets,* Appl. Anal. **101**(2022), 1715-1734.
[12] L. Cai, S. Ai, and J. Li, *Dynamics of mosquitoes populations with different strategies for releasing sterile mosquitoes,* SIAM J. Appl. Math. **74**(2014),1786-1809.
[13] J. Cariboni, D. Gatelli, R. Liska, and A. Saltelli, *The role of sensitivity analysis in ecological modelling,* Ecological Modelling **203**(2007), 167-182.
[14] Center for Disease Control and Prevention: Irradiated mosquitoes, https://www.cdc.gov/mosquitoes/mosquito-control/irradiated-mosquitoes.html, accessed on October 6, 2024.
[15] C. Castillo-Chavez, Z, Feng and W. Huang, *On the computation of $\mathcal{R}_0$ and its role on global stability,* in Mathematical Approaches For Emerging And Re-emerging Infectious Diseases: An Introduction, IMA, Vol. 125, Springer-Verlag, 2002.
[16] N. Chitnis, J. M. Cushing and J. Hyman, *Bifurcation Analysis of a Mathematical Model for Malaria Transmission,* SIAM J. Appl. Math., **67**(2006), 24-45.
[17] O. C. Collins and K. J. Duffy, *A mathematical model for the dynamics and control of malaria in Nigeria,* Infect. Dis. Model. **7**(2022), 728 - 741.
[18] A. Ducrot, S. B. Sirima, B. Somé and P. Zongo, *A mathematical model for malaria involving differential susceptibility, exposedness and infectivity of human host,* J. Biol. Dyn. **3**(2009), 574-598.
[19] A. A. El-Moamly and M. A. El-Sweify, *Malaria vaccines: the 60-year journey of hope and final success-lessons learned and future prospects,* Trop.Med. Health. **51**(1)(2023): 29.
[20] H. A. Engida, D. M. Theuri, D. K. Gathungu and J. Gachochi, *Optimal control and cost-effective analysis for leptospirosis epidemic,* J. Biol. Dyn. **17**(2023): 2248178.
[21] Fatmawata, C. W. Chukwu, R. T. Alqahtani, C. Alfiniyah, F. F. Herdicho and Tasmi, *A Pontryagin's maximum principle and optimal control model with cost-effectiveness analysis of the COVID-19 epidemic,*. Decis. Anal. **8**(2023): 100273.
[22] M. A. Ibrahim and A. Dénes, *Threshold and stability results in a periodic model for malaria transmission with partial immunity in humans,* Appl. Math. Comput. **392** (2021): 125711.
[23] International Atomic Energy Agency (IAEA), *Sterile insect technique,* https://www.iaea.org/topics/sterile-insect-technique, accessed on October 6, 2024
[24] A. Kouidere, O. Batalif and M. Rachik, *Cost-effective analysis of a mathematical modeling with optimal control approach of spread of COVID-19 pandemic: A case study in Peru,* Chaos Soliton Fract., **10**(2023): 100090.
[25] S. Lenhart and J. T Workman, *Optimal control applied to biological models,* Chapman and Hall, CRC Press, 2007.
[26] J. Li, *New revised simple models for interactive wild and sterile mosquito populations and their dynamics,* J. Biol. Dyn. **11**(2017), 316-333.
[27] S. Marino, I. B. Hogue, C. J. Ray, and D. E. Kirschner, *A methodology for performing global uncertainty and sensitivity analysis in systems biology,* J. Theor. Biol. **254**(2009), 178-196.
[28] M. Martcheva, *An Introduction to Mathematical Epidemiology*, Springer, New York, 2015.
[29] J. D. Murray, *Mathematical Biology* , 2nd edition, Springer-Verlag, Berlin, 1993.
[30] J. Mohammed-Awel and E. Numfor, *Optimal insecticide-treated bed-net coverage and malaria treatment in a malaria-HIV co-infection model,* J. Biol. Dyn. **11**(2017), 160-191.
[31] C. Ngonghala, *Assessing the impact of insecticide-treated nets in the face of insecticide resistance on malaria control,* J. Theor. Biol. **555**(2022): 111281.
[32] M. Nidhi and A. Kumar, *Assessing the impact of information-induced self-protection on Zika transmission: A mathematical modeling approach,* Comput. Math. Biophys. **12**(2024): 20230123.
[33] E. Numfor and R. Ellman, *Incorporating awareness, misinformation, and optimal control in a model of SARS-CoV-2,* J. Biol. Syst. (in revision, 2025).
[34] E. Numfor and J. Mohammed-Awel (2025), *A malaria-HIV/AIDS co-infection model with optimal treatment and insecticide-treated bednets,* in Contemporary Research in Mathematical Biology: Modeling, Computation and Analysis (edited by A. Nevai, R. S. Cantrell, M. Martcheva, S. Ruan, and Z. Shuai), World Scientific Publishing Company. https://doi.org/10.1142/12639.
[35] M. Preston, A. Carter and E. Numfor, *Modeling the effects of media awareness on SARS-CoV-2 transmission in Georgia,* Int. J. Appl. Comput. Math. **10**(2024):123. https://doi.org/10.1007/s40819-024-01759-9
[36] L. S. Pontryagin, V. G. Boltyanskii, R. V. Gamkrelize, and E. F. Mishchenko, *The Mathematical Theory of Optimal Processes,* Wiley, New York, 1962.

[37] H. Smith, Monotone dynamical systems: an introduction to the theory of competitive and cooperative systems. *AMS*, Rhode Island, 1995.
[38] John R. Silvester, *Determinants of block matrices,* The Mathematical Gazette, **84**(2000), 460-467.
[39] S. Y. Tchoumi, C.W. Chukwu, M.L. Diagne, H. Rwezaura, M. L. Juga and J. M. Tchuenche, *Optimal control of a two-group malaria transmission model with vaccination,* Netw. Model. Anal. Health Inform. Bioinform. **12**(2023): 7.
[40] Unicef Fact Sheet: Malaria vaccine price data, https://www.unicef.org/supply/media/19346/file/Malaria-vaccine-prices-09102023.pdf, accessed on February 17, 2025.
[41] Unicef Fact Sheet: Antimalarials price data, https://www.unicef.org/supply/media/7331/file/Antimalarials-prices-2019-2022.pdf.pdf, accessed on February 17, 2025.
[42] Y. Wang, J. Liu, and J. M. Heffernan, *Viral dynamics of htlv-1 infection model with intracellular delay and ctl immune response delay,* J. Math. Anal. Appl. **459**(2018), 506-527.
[43] Y. Wang, J. Liu, and L. Liu, *Viral dynamics of an HIV model with latent infection incorporating antiretroviral therapy,* Adv. Differ. Equ. **2016**(2016):225. https://doi.org/10.1186/s13662-016-0952-x.
[44] Y. Wang, Y. Zhou, F. Brauer, and J. M. Heffernan, *Viral dynamics model with ctl immune response incorporating antiretroviral therapy,* Bull. Math. Biol. **67**(2013), 901-934.
[45] World Health Organization: Malaria Fact Sheets. https://www.who.int/news-room/fact-sheets/detail/malaria, accessed on October 6, 2024.
[46] H. Yin, G. Yang, X. Zhang and J. Li *Dynamics of malaria transmission model with sterile mosquitoes,* J. Biol. Dyn. **12** (2018), 577-595.

Department of Mathematics, Augusta University, Augusta, GA 30912, USA.
Email address: enumfor@augusta.edu